NATIONAL WATER RESEARCH INSTITUTE

INSTITUT NATIONAL de RECHERCHE sur les EAUX

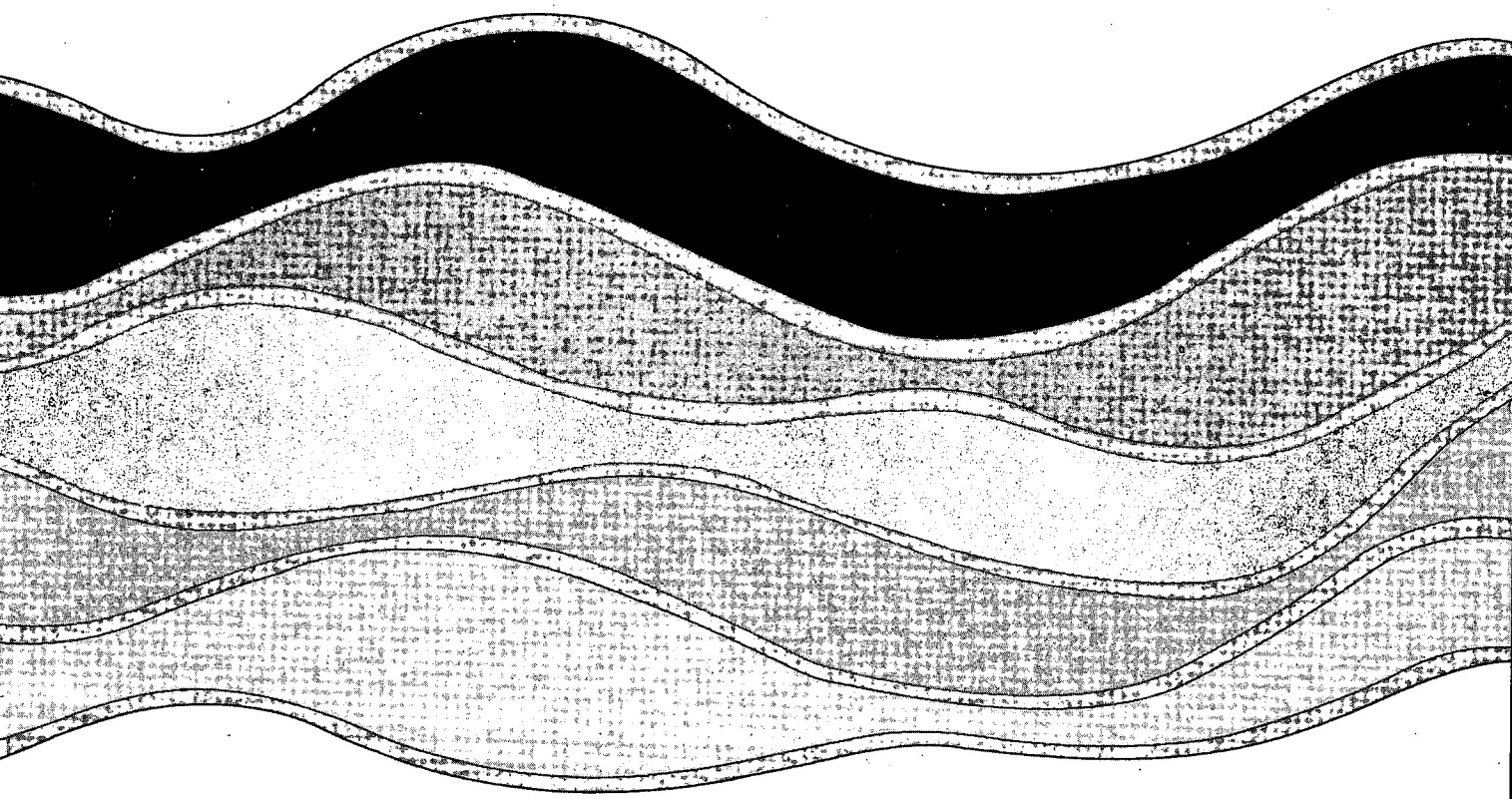

ESTIMATES OF KINETIC ENERGY DISSIPATION UNDER BREAKING WATERS

E.A. Terray, M.A. Donelan, Y.C. Agrawal, W.M. Drennan, K.K. Kahma, A.J. Williams III, P.A. Hwang and S.A. Kitaigorodskii

NWRI Contibution No. 94-57

ESTIMATES OF KINETIC ENERGY DISSIPATION UNDER BREAKING WAVES

by

E.A.Terray[1], M.A.Donelan[2], Y.C.Agrawal[3], W.M.Drennan[2], K.K.Kahma[4],
A.J.Williams III[1], P.A.Hwang[5] and S.A.Kitaigorodskii[4]

[1] *Dept. of Applied Ocean Physics and Engineering*
Woods Hole Oceanographic Institution, Woods Hole, Massachusetts, U.S.A.

[2] *National Water Research Institute*
Canada Centre for Inland Waters, Burlington, Ontario, Canada

[3] *Northwest Research Assoc. Inc., Bellevue, Washington, U.S.A.*

[4] *Finnish Institute of Marine Research, Helsinki, Finland*

[5] *Quest Integrated Inc., Kent, Washington, U.S.A.*

Revision dated 5 April, 1994

Corresponding author : Dr. M.A. Donelan, Canada Centre for Inland Waters, Box 5050, 867 Lakeshore Rd., Burlington, Ontario L7R 4A6

MANAGEMENT PERSPECTIVE

The mixing of surface waters by wave action bears directly on many practical problems and phenomena associated with the use of lakes as a resource; e.g. the dispersal of buoyant pollutants (sewage, oil spills); gas transfer across the air-water interface; nutrient mixing; photosynthetic efficiency of plankton. This study reveals new information on the structure of the turbulence in the upper layers beneath breaking waves. It is shown that the dissipation rates of kinetic energy are many times larger than the traditional estimates. A structure for the near surface layers is described and may be used for modelling in lakes and oceans.

SOMMAIRE À L'INTENTION DE LA DIRECTION

Le mélange de la couche superficielle d'eau sous l'action des vagues a des effets directs sur de nombreux problèmes et phénomènes associés à l'utilisation des lacs comme ressource. Ainsi, on peut penser à la dispersion des panaches de contaminants flottants (eaux d'égout, pétrole déversé), aux échanges gazeux à l'interface air-eau, à la circulation des nutriments comme à l'efficacité de la photosynthèse planctonique. Cette étude apporte de nouvelles connaissances sur la structure de la turbulence dans les couches supérieures d'eau sous les vagues déferlantes. On y montre que les taux de dissipation de l'énergie cinétique sont plusieurs fois supérieurs aux estimations classiques. On y décrit une structure des couches proches de la surface qui peut servir à des travaux de modélisation pour les lacs et les mers.

ABSTRACT

The dissipation of kinetic energy at the surface of natural water bodies has important consequences for many physical and biochemical processes including wave dynamics, gas transfer, mixing of nutrients and pollutants and the photosynthetic efficiency of plankton. Much attention has been focused on the measurement of kinetic energy dissipation in the upper mixed layer but relatively little reliable information is available in the near surface wave zone. Although several experimental results are in general agreement with dissipation rates following wall layer theory, our results clearly indicate that under breaking wave conditions there is a near surface zone of enhanced dissipation – well above that predicted by wall layer theory. Here we provide a scaling law for the rate of dissipation based on wind and wave parameters, and conclude that the dissipation rate under breaking waves depends on depth, to varying degrees, in three stages. Very near the surface, within one significant height, the dissipation rate is high and roughly constant. Below this is an intermediate region where the dissipation rate is high, an order of magnitude greater than that predicted by wall layer theory, and rapidly decaying (z^{-2}). The thickness of this layer is proportional to the normalized (by ρu_*^3) energy input to the water column due to breaking which, for waves with $U/c_p > 2$, is proportional to wave age. At sufficient depth the dissipation rate asymptotes to values commensurate with traditional wall layers. The total energy flux into the column is several times greater than the conventional estimate of $\rho u_*^3/2$ and depends strongly on wave age. These results imply a pronounced shift in our approach to measuring kinetic energy dissipation in wave-stirred regions and in the modelling of various physical, chemical and biological processes.

RÉSUMÉ

La dissipation de l'énergie cinétique à la surface de plans d'eau naturels a d'importantes conséquences sur de nombreux processus physiques et biochimiques, notamment la dynamique des vagues, les transferts gazeux, la circulation des nutriments et des contaminants ainsi que l'efficacité de la photosynthèse planctonique. La mesure de la dissipation de l'énergie cinétique dans la couche mixte supérieure a été beaucoup étudiée, mais il y a assez peu de connaissances fiables sur la couche superficielle contenant l'oscillation de surface. Même si plusieurs résultats expérimentaux s'accordent en général avec les taux de dissipation prévus par la théorie de la «wall layer», nos résultats montrent clairement qu'en conditions de vagues déferlantes, il se forme une couche superficielle de dissipation accrue, beaucoup plus près de la surface que ce que laisse prévoir cette théorie. Nous proposons ici une loi d'échelonnage qui s'applique au taux de dissipation compte tenu du vent et de paramètres associés aux vagues. Nous parvenons à la conclusion que le taux de dissipation sous des vagues déferlantes dépend de la profondeur, à différents degrés et en trois couches. Très près de la surface, dans l'espace qui correspond à une hauteur caractéristique, le taux de dissipation est élevé et à peu près constant. Au-dessous se trouve une couche intermédiaire où le taux de dissipation est élevé, soit une ordre de grandeur de plus que celui prévu par la théorie de la «wall layer» et où il s'amenuise rapidement (z^{-2}). L'épaisseur de cette couche est proportionnelle à l'énergie normalisée (par ρu^3_*) communiquée à la colonne d'eau par le déferlement qui, pour des vagues à $U/c_p>2$, est proportionnel à l'âge de la lame. À une profondeur suffisante, la courbe du taux de dissipation prend la forme d'une asymptote à des valeurs compatibles avec les «wall layers» classiques. Le flux énergétique total dans la colonne est plusieurs fois supérieur à l'estimation classique de $\rho u^3_*/2$ et dépend fortement de l'âge de la lame. Ces résultats laissent prévoir un changement profond dans notre façon de mesurer la dissipation de l'énergie cinétique dans les couches agitées par les vagues, ainsi que dans notre façon de modéliser différents processus physiques, chimiques et biologiques.

1. Introduction

The rate of turbulent kinetic energy dissipation (ϵ) in the upper oceanic layers and, in particular, its distribution near the surface are of great significance in matters relating to the mixing of near surface waters, mass transfer across the interface, dispersal of buoyant pollutants, testing of similarity hypotheses related to turbulent structure and the modeling of thermocline development, inter alia. It is therefore not surprising that in recent years a great deal of effort has been directed toward determining its near-surface vertical distribution. Estimates of dissipation near the top of the water column have been made from three distinctly different types of platforms, *viz.*: (i) fixed towers; (ii) horizontally or nearly horizontally moving vehicles (ships, submarines, and towed bodies); (iii) vertically profiling devices driven by a buoyancy difference. Only in very rare cases has the dissipation been estimated from the smallest scales where conversion of mechanical energy to heat occurs. Much more usually the spectral density at intermediate scales is employed, via the Kolmogorov similarity hypothesis, to estimate the rate at which energy flows from the (large scale) source to the (small scale) sink. Occasionally, dissipation is inferred indirectly on the basis of some assumption about the energy budget – for example, that shear production and dissipation are in balance. Most measurements have been made beneath the wave zone, although a few have explored the topmost few meters. Furthermore, most measurements have been made in light and modest winds, but a (very) few have been acquired in strong winds and breaking waves.

The interpretation of surface layer dissipation estimates falls into two broad classes: (i) general agreement with the structure of a classical wall layer as expressed by similarity scaling; (ii) much higher dissipation values than expected from a purely shear driven wall layer, and usually attributed to wave breaking. The evidence from individual campaigns is at best fragmentary. Given the highly intermittent nature of the small scale process of energy dissipation and of one possible source of kinetic energy (wave breaking) and the very short observing times leading to most of the reported dissipation estimates, the order of magnitude agreement between estimates (in similar conditions) and with wall layer scaling is hardly surprising, but thoroughly inconclusive (*cf.* Agrawal *et al.*, 1992).

It is the purpose of this paper to examine an extensive series of tower based data,

obtained under a variety of atmospheric forcing conditions, to attempt to find the sources of energy dissipation at the top of the water column and to parameterize the latter in terms of appropriate atmospheric forcing and wave parameters.

2. Previous Work

The first measurements of dissipation in the ocean were made by Grant *et al.* (1962) in a tidal channel. This classical work is credited with verifying the Kolmogorov inertial subrange hypothesis. Subsequently, Stewart and Grant (1962) applied the same methods to estimate dissipation near a wind forced sea surface. They report nine estimates of ϵ taken over a depth range of 1-15 m, and the rather restricted wind speed range of 7-10 m s^{-1}. They note "a rather weak dependence on depth near the surface and the expected increase of ϵ with wave height." If expressed in wall coordinates the data scatter from about 0.4 to 7 times the expected wall layer value, $u_{*w}^3/\kappa z$ (u_{*w} is the friction velocity in the water, z the depth, and κ von Karman's constant, 0.4). Stewart and Grant assume that the energy input from the wind is delivered to the dominant waves, and estimate the energy flux as τc_p, where τ is the wind stress and c_p the phase speed of waves at the spectral peak. They find that this estimate is more than an order of magnitude greater than the depth-integrated dissipation from 1 m to 15 m, and infer that "almost all wave dissipation is concentrated very near the surface, essentially above the trough line". We remark that their calculation of the wind input is an over-estimate since the form drag on the waves is distributed across the wave spectrum, leading to an estimate of the wind input as $\tau_w \bar{c}$ rather than τc_p, where τ_w denotes the wave drag, and $\bar{c}$ is an average phase speed over the slope spectrum of the waves (*i.e.* the roughness elements). Although τ_w is somewhat less than τ, we will show in a later section that $\bar{c}$ is substantially less than c_p for waves approaching full development.

By far the most common approach to estimating dissipation in the ocean is via the use of automatic vertical profiling devices carrying velocity or temperature microstructure probes (Dillon *et al.*, 1981; Oakey and Elliott, 1982; Soloviev *et al.*, 1988; Gregg 1987; Gargett, 1989; Anis and Moum, 1992). The first three studies are in general agreement with wall layer scaling, whereas the last three report significantly higher near-surface dissipation

rates. However, the data of both Dillon *et al.* and Soloviev *et al.* were obtained at low wind speeds (less than 6 m s $^{-1}$), and the observations of Oakey and Elliot were taken mostly below the wave zone. Given the sporadic nature of the injection of turbulence by wave breaking, the short residence time of vertical profilers in the wave zone, and the well-known intermittency of dissipation fluctuations, it is clear that only studies specifically designed to sample the near-surface layer, and including a very large number of profiles (e.g. Anis and Moum, 1992), are likely to achieve statistically stable estimates of dissipation in this region (Agrawal *et al.*, 1992).

Towers are particularly well suited platforms for exploring the wave zone, since they provide the stable support necessary for acquiring the long time series necessary to sample breaking adequately. Their principal drawback is that the advection velocity is not imposed and may be very weak and variable, thereby introducing a source of error if ϵ is estimated via the spectral density in the low frequency (*i.e.* below the wave peak) inertial sub-range. However, as discussed in the next section, reliable estimates can be derived from the inertial subrange at frequencies above the wave band. The tower estimates of ϵ reported to date are those of Arsenyev *et al.* (1975), Kitaigorodskii *et al.* (1983) – referred to subsequently as KDLT – and Jones (1985). Arsenyev *et al.* estimated ϵ by measuring the stress and the velocity gradient and assuming equality of shear-generated production and dissipation. Their data were collected in relatively calm conditions ($\overline{U} \sim 6$ m s^{-1}). KDLT and Jones estimated ϵ from the spectral density of velocity components in the inertial sub-range, and both authors include winds over 10 m s^{-1}. KDLT report dissipation estimates more than an order of magnitude above that given by wall layer scaling, whereas Jones claims agreement with the wall layer form, $u_{*w}^3/\kappa z$, although his strongest wind case exceeds this by a factor of 5 and (in his Fig.3) approaches the estimates of KDLT.

Finally, we mention the very interesting observations obtained by Osborn *et al.* (1992) on the California shelf, east of San Clemente Island, using a microstructure shear probe mounted on a submarine. These authors found cases of enhanced dissipation during periods of moderate winds but active breaking that were correlated with the penetration of bubble clouds. A horizontal spatial average yielded dissipation profiles that exceeded wall layer predictions by an order of magnitude to depths of more than 5 m.

It is clear from this brief review that the observational picture is not yet clarified. Although older observations generally support the wall layer analogy, more recent studies designed to explore the very near-surface region have found higher dissipation rates. Furthermore, many researchers, even while claiming order of magnitude agreement with wall layer scaling, allow that wave breaking must be an important source of kinetic energy very near the surface, and of momentum to the deeper currents. Hence, there must be a layer whose scaling is controlled by the various characteristics of the wave field, such as its state of development. As one moves away from the surface the direct effect of the waves diminishes, and at some depth it is not surprising that wall layer scaling appears to describe the observations adequately. The principal issues, then, are: How may these two regions be consistently described? What are the appropriate scaling variables or combination of variables for the wave-dominated layer? It was to answer these questions, and others associated with turbulence near the air-water interface, that an extensive field observational program was put in place in Lake Ontario in three successive autumns (1985-1987). The program was entitled "Water Air Vertical Exchange Studies" (WAVES). The principal players were the National Water Research Institute (the host institute), the Woods Hole Oceanographic Institution, the Finnish Institute of Marine Research, the Johns Hopkins University and the U.S. Naval Research Laboratory.

3. The Measurements

The choice of experimental site was based on several criteria. Among them were: (a) a rigid platform with minimal disturbance to the flow of either air or water near the interface; (b) good supporting measurements of wave directional properties and meteorological information including wind stress; (c) climatology commensurate with a respectable range of wind speeds up to at least 15 m s^{-1}. The air-water field facility of the Canada Centre for Inland Waters (CCIW) provided an ideal site for these measurements. The tower (Fig.1) is rigidly fixed to the bottom in 12 m of water at the western end of Lake Ontario. It is 1.1 km from the shore so that the prevailing south-westerlies approach it at very short fetch (Fig.2). This is useful because the resultant strong forcing near the peak tends to produce effects of breaking that are felt well below the trough level. On the other hand east and north-east winds, which are not uncommon in the fall, may build up substantial

waves over the long fetch of the lake (300 km). Waves of 3.5 m significant height have been recorded at the tower and, on occasion, much larger waves have swept equipment off the upper deck some six meters above mean water level.

The tower was designed for waves and air-water interaction research and thus there is a minimum of interference to flow near the interface. The tower structure disturbs the interfacial layers (from 3 m above the surface to 6 m below) only with 4 legs of 41 cm diameter and a rotatable mast of ellipsoidal cross-section (28.5 cm × 18 cm), on which current meters were mounted. The tower was also equipped with a full set of instrumentation for estimation of the mean environmental conditions, wind stress and heat flux. A detailed picture of the wave directional properties was provided by an array of six capacitance wave gauges mounted on the north side of the tower (Tsanis and Donelan, 1989). Most signals were digitized on the tower and transmitted to the shore station via underwater cable, so that recordings could be made in any weather without the necessity of gaining access to the tower. This capability also permitted us to remotely position various of the instruments.

During the entire experiment a wide range of conditions were observed including: wind speeds from 3 m s^{-1} to 17 m s^{-1} (lower wind speeds were generally too variable to permit analysis via Reynolds' averaging techniques); significant wave heights from a few centimeters to 2.5 m; mean current speeds from 2 cm s^{-1} to 20 cm s^{-1}, and wave development ranging from swell to very young, short-fetch, waves. In the analysis and interpretation of our earlier work at the same site (KDLT) we realized that, in order to acquire convergent second-order statistics of the velocity field, it was necessary to gather fairly long (20 minutes or more) time series at a particular depth. Consequently, we chose to employ many fixed instruments and to space them out over a suitable depth range.

The data reported here were obtained from three completely different types of current meters: (a) miniature Dragsphere devices, in which the vertical and one horizontal component of velocity are obtained from a measurement of the instantaneous force on a 4 mm sphere attached to the end of a 0.4 mm diameter rod (Donelan and Motycka, 1978), (b) "BASS" acoustic travel-time current meters (Williams, 1985), and (c) a 2-axis

laser-Doppler velocimeter (Agrawal and Belting, 1988).

The Dragspheres were designed to sense velocity fluctuations with wave lengths as small as 2 cm, and were sampled at 20 Hz. During 1985 there were 3 Dragspheres spaced vertically in the upper 4 meters; in 1986 and 1987 we deployed two of these devices in the upper 2 meters. BASS measures velocities along four directions arranged as orthogonal pairs in orthogonal planes. Each acoustic path is a cylindrical tube having a diameter of approximately 1 cm and a length of 15 cm. Velocity measurements were taken at 20 Hz, averaged internally, and recorded at 5 Hz. In all three years 12 acoustic current meters were installed, spaced at approximately half meter intervals over the top 6 meters. The Dragspheres and acoustic current meters were mounted in a vertical plane on the west face of the tower, pointing outwards on opposite sides of the minor axis of the ellipsoidal mast. The 4 mm spheres and the sensing volume of the acoustic current meters were about 1.5 m on either side of the mast. Forty-five centimeters closer to the mast were two wave staffs, one on either side. The wave staffs were used to estimate the propagation direction of the waves, and this information then used to set the azimuthal orientation on the current meters so as to minimize the flow component across the mast. The laser Doppler velocimeter (LDV) was deployed in the 1986 and 1987 field seasons. It measured the vertical and east-west horizontal velocity components, and was sampled at a rate of 128 Hz. The LDV was mounted on a vertical profiler having 1 meter of travel. The profiler was separated by 12 m from the ellipsoidal mast holding the other current meters. Time series of 256 seconds duration were collected at a sequence of four depths separated by 10 cm. Another capacitance wave staff was located at the LDV to provide a local measurement of wave height (this staff was displaced laterally by 30 cm from the sampling volume).

The miniature Dragspheres were difficult and costly to construct and very fragile so that, while we began the experiment with three fully functional instruments, we concluded after three seasons with a single serviceable one. Their gains were carefully calibrated before and after each field season in the 100 m towing tank at the Canada Centre for Inland Waters (CCIW). Because the force components measured by the Dragsphere depend quadratically on the water velocities, the estimation of both mean and fluctuating velocity

components is affected by the quiescent ('zero') output of the instrument. This was acquired in the field at the beginning and end of each run (usually 90 minutes long) by remotely positioning a cylindrical sleeve over each instrument. Any significant difference between these pre- and post-run zeros (obtained from 5 minute averages) would cause rejection of that data set. Small differences were removed by subtracting a linear trend through the pre- and post-run zeros from the run data. During the 1985 field season, the Dragspheres consistently showed excellent agreement (within 7%) with linear theory (see Drennan *et al.*, 1992a). During the much longer 1987 field season, however, fouling of the Dragspheres due to algal growth caused a gradual increase in drag area. The 1987 Dragsphere data have therefore been recalibrated so as to agree with linear theory in the vicinity of the wave spectral peak.

The acoustic current meters were at a more advanced stage of development and were employed in a greater number. The sensors together with their associated electronics were mounted on two lengths of aluminum channel, and were deployed by fastening the channel sections to the rotatable mast at the tower. Pre- and post-field zero offsets, which were measured in the laboratory with the sensors and cables attached to the channels, agreed to within 0.5 cm $^{-1}$. The gain of the acoustic current meters depends only on the probe geometry and the speed of sound. Nonetheless, at the end of the experiment we verified both the nominal gain and the cosine response of these sensors in the CCIW 100 m towing tank. Since both the BASS and Dragspheres are *in-situ* instruments, the question of flow disturbance is a critical one for their performance. To investigate this issue we conducted extensive tests of both instruments in the 100 m wind-wave flume at CCIW under mechanically–produced waves and currents having magnitudes comparable to those observed in the field. The BASS and Dragsphere measurements agreed closely with each other as well as with external measurements of the flow (the wave velocity was deduced from surface displacement using linear theory), even when the *rms* orbital velocity exceeded the mean current by an order of magnitude. We also conducted runs with the BASS positioned at various distances from a replica of the ellipsoidal mast used to support the instruments in the field. Although a 10% perturbation of the mean flow was measured, there was no measurable increase in spectral levels at frequencies above the wave band.

4. Experimental Results

We use Kolmogorov's similarity hypothesis to estimate ϵ from the magnitude of the velocity spectra in the inertial subrange of wavenumbers. In the case of steady advection, the connection to the more easily measured frequency spectrum is commonly made via the well-known Taylor "frozen turbulence" hypothesis, which relates the radian frequency and wavenumber via the mean advection or drift, U_d, as $\omega = U_d k$. Then the dissipation rate can be estimated as

$$\epsilon = C U_d^{-1} [S(\omega)\omega^{5/3}]^{3/2} \qquad [1]$$

where $S(\omega)$ is the one-sided frequency spectrum of velocity evaluated in the range of frequencies exhibiting a $-5/3$ spectral slope. The numerical value of the constant C is either 2.9 or 1.9 depending on whether the direction of the velocity component is in line with or normal to the mean flow, U_d. Lumley and Terray, (1983), have shown that a similar result applies when the advection is due to a combination of waves and currents in which the *rms* wave velocity exceeds the mean. In this case, equation [1] continues to hold for frequencies in the inertial subrange below the wave peak. However, above the wave band, U_d is given by the *rms* wave orbital velocity at the observation depth (note that [1] is then the leading term in an expansion in the ratio of the local mean to *rms* velocity). Lumley and Terray (in their Appendix A) analyzed the advection of isotropic turbulence by deep water waves having a narrow directional distribution. Defining U_d as $\sqrt{2}$ times the *rms* vertical wave velocity, they found that $C \simeq 2.7$. They further showed that, as a consequence of the circularity of the wave orbits, horizontal and vertical velocity spectra are equal at high frequencies (in contrast $S_w = \frac{4}{3} S_u$ for rectilinear advection).

The existence of $-5/3$ regions in the frequency spectra of velocity, both above and below the wave band, has been demonstrated by a number of studies (Jones and Kenney, 1977; Kitaigorodskii *et al.*, 1983; Jones, 1985). From the large data base of the WAVES experiment we show some examples in Figs. 3a and 4a. Although not all velocity spectra show well-established $\omega^{-5/3}$ regions, most do and these are typical of those that do. The spectra of Figs. 3a/4a are displayed again in Figs. 3b/4b, multiplied by $\omega^{5/3}$. Both horizontal and vertical velocity spectra have $-5/3$ regions above the wave peak, whereas

only the horizontal velocity spectra show $-5/3$ regions at low frequencies due to the suppression of long wavelength vertical velocity fluctuations by the surface. The occurrence of this behavior at low frequencies is interesting in its own right, and points to the existence in the surface layer of energy-containing fluctuations that are considerably more anisotropic than their counterparts in shear flows over fixed boundaries, such as the atmospheric surface layer over land. However, for the very low mean advection velocities typical of the WAVES data set, the spatial structure of these eddies is confused with their dynamical evolution, and therefore the low frequency part of the horizontal velocity spectrum cannot be used reliably to estimate dissipation. Furthermore, since the likelihood of the condition of isotropy being satisfied is much greater for high frequencies, we have exclusively used the region above the wave band to estimate spectral levels.

It is clear that the turbulent $-5/3$ regions extend well beyond the wave peak and hence are not affected by the wave orbital velocities. This can be seen in Figs. 3a/4a where we have applied linear theory to the surface elevation measured at the nearby wave-staffs to estimate the spectrum of vertical wave velocity. We may therefore, without recourse to filtering out the wave-induced motion, treat the spectra outside of the wave band as a reflection of the turbulence properties. Soloviev *et al.*, (1988), have suggested that the very high dissipation rates reported by KDLT are spurious and may be due to limitations in the linear filtration technique used. This is clearly not so, since whatever the drawbacks of linear filtration, its application does not alter the spectra in the $-5/3$ regions well apart from the wave-dominated central region. KDLT applied the linear filtration approach specifically to investigate the structure of turbulence over the entire spectrum, including the wave band. Here we wish to explore the dissipation rate only, and therefore focus our attention on the outer limits of the spectrum where application of linear filtration is clearly unnecessary. Thirty-six pairs of estimates of ϵ from the high frequency regions of BASS data are compared in Fig. 5. The range of ϵ covers $2\frac{1}{2}$ decades and exhibits good agreement between the estimates from either component – the Dragsphere results show similar agreement.

In as much as dissipation estimates are affected by flow disturbances around the velocimeter, particular attention has been paid to identifying and eliminating various

sources of flow disturbance. This was a major factor in the design of the tower, and also in the implementation of the experiment. Several criteria were employed in the selection of the data for inclusion in this work. First of all, only west wind cases were used. Not only are the BASS and Dragspheres on the windward side of the tower in these cases, but the wind waves are strongly fetch limited, with significant wave heights less than 50 cm and minimal likelihood of turbulence being generated from the legs of the tower. Initially, many east wind cases were analyzed, and for these, the typical significant wave height was around 1–2 m. However, with such large orbital motions, and with the Dragsphere and BASS instruments on the leeward side of the tower, it was thought that the potential for flow disturbance at the measuring sites was high. Hence, the east wind cases were omitted from the final set of runs analyzed here. A second criterion was that the mean current (as measured by BASS) be in the downwind direction – that is, perpendicular to the Dragsphere-mast-BASS axis. On runs where the current ran along the axis from the BASS units towards the Dragsphere, the Dragsphere inertial subrange energy levels were found to be elevated above those of BASS presumably due to the effects of the mast. Such runs were omitted from the final data set. We note that the preliminary results presented earlier (Drennan *et al.*, 1992b) were based on the Dragsphere data alone and consequently contained some points which have been now been rejected on the basis of the mean current (BASS) criterion.

The dissipation estimates from the BASS and Dragsphere were obtained from 90 minute records using the relation [1], averaged over a bandwidth of several Hz (the actual bandwidth varied with each instrument and from run to run). Based on the statistics of the spectral estimates, the standard error in dissipation is approximately 1%. The Dragsphere has a spherical sampling volume, approximately 0.4 cm in diameter, and was sampled at 20 Hz. Velocity spectra obtained from it typically have a well-developed $\omega^{-5/3}$ region spanning a decade or more in frequency. Although BASS was sampled at 20 Hz, the output was averaged and recorded at the lower rate of 5 Hz, resulting in a smaller range of frequencies that could be used to determine the spectral level. Nonetheless, it is apparent from Table 2 (see also Fig. 7) that these two instruments agree to within the scatter of the data.

The LDV measurements were acquired as repeated 256 s records at depths of 20, 30, 40 and 50 cm, so that the data listed in Table 2 represent an observation period of slightly less than 20 minutes at each depth. Although measurements from the three lower depths were essentially continuous, the dropout rate at 20 cm was roughly 10% (presumably because of the occasional interruption of the beams during passage of the higher waves). Simulation has indicated that this level of dropout can significantly affect the spectrum at high frequencies, and for this reason we have excluded the 20 cm observations from the data reported here. An estimate of dissipation was obtained for each 256 s record from the level of the vertical velocity spectrum in the inertial subrange. The four individual estimates of dissipation at each depth were then averaged to obtain the result given in Table 2. The standard error of the average of the four estimates is roughly 130%. While some individual 256 s records yield dissipation rates in agreement with those observed by the Dragspheres and BASS, the averaged LDV results lie below the other two sensors (although they have roughly the same logarithmic slope). We have considered several explanations for this discrepancy, but have not found an entirely convincing reason for the systematic difference.

5. Dissipation Rate Scaling

Soloviev *et al.* (1988) have argued that the appropriate physical variables for describing the scaling of ϵ in the upper ocean are the friction velocity, u_{*w}, depth, z, and gravitational acceleration, g. The wind action is reflected in u_{*w} and g is intended to account for the presence of surface gravity waves at the interface. They continue their development by using dimensional analysis to suggest that $\epsilon z/u_{*w}^3$ should be a function solely of gz/u_{*w}^2.

This approach embodies several limitations. First, Soloviev *et al.* have restricted their discussion to the case of full development. This results in their use of u_{*w}^2/g, which is proportional to the wave height at full development, as a length scale. However, it is likely that this scale may be a substantial overestimate when the waves are not fully developed. Second, the apparent agreement with wall layer scaling cited by Soloviev *et al.* requires that the layer in which wave breaking dominates lies above their observed depths. They justify this by referring to Csanady (1984) and conclude that all measurements cited, including

those of KDLT (and of this study) are made below the wave-breaking zone. However, Csanady's estimates of the depth of the well-mixed layer due to breaking were based on observations of drifters in relatively calm seas disturbed primarily by breaking wavelets. Furthermore, the full data set he presents does not yield a single breaking zone depth but, in fact, a range of depths covering almost two orders of magnitude, from $zg/u_{*w}^2 \approx 1.3 \times 10^{-5}$ to 1.7×10^{-7}. Clearly a well defined transition depth does not arise using the Soloviev *et al.* depth coordinate. A final objection, pointed out in Agrawal *et al.* (1992) is that the WAVES data, involving strong forcing and under-developed waves, do not collapse under the Soloviev *et al.* scaling. We believe that all of these considerations point strongly to the need to take explicit account of wave development in the parameterization of upper layer turbulence.

On the other hand, whereas KDLT, Agrawal *et al.* (1992), and others have found enhanced dissipation close to the surface, it is clear from the data compiled by Soloviev *et al.* that sufficiently far from the air-sea interface the dissipation rate is similar to that observed in shear flows over solid boundaries. Our objective here is to propose a framework that encompasses these, apparently dissimilar, observations, and that gives a quantitative measure to the notion of "sufficiently far".

The scaling we propose below is based on two physical hypotheses. First, we assume that at high wind speeds wave breaking is the principal source of turbulent kinetic energy in the near surface layer, and second that the thickness of the layer in which the energy is initially deposited (*i.e.* the region that is directly stirred by the breaking) is proportional to wave height. These two propositions, although not unique, are consistent with our data and lead to specific predictions concerning the vertical structure of dissipation close to the surface that are amenable to experimental verification.

The justification for the first hypothesis lies in the observation that when the surface is aerodynamically rough (this condition depends on wave development, but corresponds approximately to wind speeds above 8-9 m/s) the energy and momentum fluxes from the wind to the water are transmitted by normal stresses on the roughness elements themselves (*i.e.* to the waves). Because the waves are known to retain only a small fraction of these

fluxes (Hasselmann et al., 1973; Donelan, 1978; Mitsuyasu, 1985), it follows that, regardless of the spectral distribution of wave dissipation, the vertically-integrated dissipation rate in the water will be proportional to the mean energy flux from the wind to the waves. Given the unsatisfactory state of our present understanding of the spectral distribution of wave dissipation (Hasselmann, 1974; Phillips, 1985; Donelan and Pierson, 1987), this presents an essential simplification, and is central to the discussion that follows.

Support for our second hypothesis is more tenuous. It is known, based on the laboratory results of Rapp and Melville (1990) concerning the breaking of focused wave packets, that the immediate production of turbulence extends to depths of order of the height of the breaking wave, that is, the maximum superposed height of the group. Although breaking over a wind-generated spectrum of waves is undoubtedly more complex (for example, fluctuations in wind forcing may be dissipated quasilocally in wavenumber by short waves that are strongly coupled to the wind), the breaking of waves near the peak of the spectrum (which are generally weakly coupled to the wind) almost certainly involves superposition, and hence should be closely related to the mechanics elucidated by Rapp and Melville. Since the energy and momentum fluxes per breaking event increase with increasing wavelength, the maximum depth of direct injection is therefore likely to be determined by the breaking of waves around the peak of the spectrum (the direct stirring by shorter breaking waves will be nested within the dominant scale), and hence we expect the significant height of the wind-waves, H_s, to provide a suitable choice of vertical scale.

We begin by defining a normalized wind input, F_w, such that $\rho_w F_w$ is the energy flux from the wind to waves. Note that this normalization is in keeping with the usual definition of ϵ as the rate of energy dissipation per unit mass. In deep water, we expect the dissipation rate to be a function of z, u_*, H_s, c_p, k_p, and F_w (for the unstratified case under consideration here the air and water densities can enter only as a ratio, whose principal role is to relate the corresponding friction velocities – consequently we will henceforth drop explicit reference to density and use either friction velocity interchangeably, distinguishing them when necessary by means of the subscripts 'a' and 'w'). Note also that while the gravitational acceleration, g, does not appear, it is implicit in the dispersion relation which links k_p and c_p. Following our previous discussion, we choose to non-dimensionalize the

dissipation rate by F_w and H_s. Based on dimensional analysis, the normalized dissipation must then be a function of four dimensionless variables, which we take to be the ratios z/H_s, c_p/u_*, $F_w/u_*^2 c_p$, and $k_p H_s$. In the case of fetch-limited waves it is conventional practice to parameterize the state of wave development in terms of wave age, c_p/u_*, (Donelan *et al.*, 1985). Accordingly, the last two variables, wave steepness and normalized energy flux, can be dropped since they are expressible as functions of wave age. Note that this argument also applies to other dimensionless combinations of wave variables, such as the normalized spectral bandwidth, *etc.* Although strictly speaking a description purely in terms of wave age must be an approximation, we believe that it captures the main features of the development of the wave spectrum that are important in determining the energy flux through the air-sea interface.

Based on the above arguments, a scaling law for upper layer dissipation under breaking wave conditions can be written as:

$$\frac{\epsilon H_s}{F_w} = f(z/H_s, c_p/u_{*a}), \qquad [2]$$

where f is a function to be determined from the data, and we have chosen the conventional definition of wave age in terms of the air-side friction velocity. Although this expression depends on two variables, the WAVES data suggest that when scaled in this way, there is a range of depths near the surface over which the non-dimensional dissipation rate is independent of wave age. We note in passing that this cannot be true everywhere, since a dependence on c_p/u_{*a} is required in order to recover the observed wall-layer scaling (*i.e.* $\epsilon z/u_{*w}^3 = const.$) at greater depths.

Before proceeding, it is useful to determine the dependence of the wind input on wave age. The rate of energy input to the waves from the wind, F_w, is defined as the integral of the growth rate, β, over the wave spectrum, where β is the e-folding scale for the temporal growth of wave energy in the absence of non-linear interactions and dissipation. Then:

$$F_w = g \int \frac{\partial S_\eta}{\partial t} d\omega d\theta = g \int \beta S_\eta d\omega d\theta, \qquad [3]$$

where $S_\eta(\omega, \theta)$ is the frequency-direction spectrum of the waves. There is general

agreement, based on both theory (Jeffreys, 1924, 1925; Miles, 1957) and experiment (Plant, 1982), that β is quadratic in either wind speed or friction velocity. We use a formulation due to Donelan and Pierson (1987) that relates β at each frequency to the wind speed as:

$$\frac{\beta}{\omega} = 0.194 \frac{\rho_a}{\rho_w} \left(\frac{U_{\pi/k} \cos\theta}{c(k)} - 1 \right) \left| \frac{U_{\pi/k} \cos\theta}{c(k)} - 1 \right| \qquad [4]$$

where for a wave component of wavenumber $\vec{k}$, having phase speed $c(k)$, both the magnitude, U, and direction, θ, of the wind are evaluated at a reference height of π/k (*i.e.* at one-half the wavelength).

We can define an "effective phase speed", $\bar{c}$, related to wind input, by parameterizing F_w in terms of this speed and the wind stress, τ_a, as:

$$F_w \equiv \tau_a \bar{c} / \rho_w \simeq u_{*w}^2 \bar{c}, \qquad [5]$$

where we have made use of the approximate equality between the wind stress and the surface value of the turbulent stress in the water, $\tau_a \equiv \rho_a u_{*a}^2 \simeq \rho_w u_{*w}^2$ (this relation follows from our assumption that the entire wind stress is supported by the waves, and the fact that only a few percent of the applied stress is necessary to account for the observed growth of the waves with fetch).

As defined in [5], $\bar{c}$ is the characteristic velocity associated with the energy flux and arises from contributions over the entire spectrum. At one extreme of wave development that is realized in laboratories it approaches the peak wave velocity, while at the other, near full development, it is of the order of the friction velocity u_{*a}. We have computed $\bar{c}$ using equations [3], [4] and [5] for a wide variety of observed wave spectra drawn from both the WAM database (Kahma and Calkoen, 1992), and this experiment. The results, normalized by the phase speed at the peak of the wave spectrum, are shown in Fig. 6 as a function of inverse wave age, u_{*a}/c_p. In order to calculate the integral in [3], the observed spectra were extended to frequencies beyond $3.5 \times \omega_p$ by appending an ω^{-5} tail. This form for the equilibrium range of the spectra is consistent with observations once the Doppler shift due to the orbital velocities of the long waves has been removed (Banner, 1990). Since most of the WAM data base does not include measurements of wave direction, we carried

out the angular integrations in [3] using the parametric form of the directional distribution, $sech^2(\alpha\theta)$, proposed by Donelan *et al.*, (1985). The dominant frequency contribution to [3] comes from the rear face of the spectrum, where the directional spread of the waves is large (in this region $\alpha \approx 1.2$ and the *rms* directional spread is roughly 40 degrees). As a result, our calculation is not especially sensitive to the particular choice of angular distribution. Friction velocities in the air were calculated using the relation:

$$u_{*a} = \kappa \frac{U_{10}}{\ln(10/z_o)} \qquad [6]$$

The roughness length, z_o, needed in [6], was computed from an empirical regression based on previous meteorological observations taken at the WAVES site (Donelan, 1990):

$$\frac{z_0}{H_s} = 1.38 \times 10^{-4}(\frac{U_{10}}{c_p})^{2.66}. \qquad [7]$$

Figure 6 shows that $\overline{c}$ is roughly 10% of c_p near full development, but that it rises quickly to a fairly constant value of 50% for u_{*a}/c_p larger than 0.075. Although Fig. 6 includes the entire range of wave development encountered during WAVES, the subset used here to determine the dissipation rate all have $\overline{c}/c_p$ approximately 0.5.

As a consistency check, we repeated the above calculation using the form for β given by Plant (1982):

$$\frac{\beta}{\omega} = 0.04(\frac{u_{*a}}{c(k)})^2 \cos\theta, \qquad [8]$$

The results for $\overline{c}/c_p$ closely follow those shown in Fig. 6, although they are roughly 20% higher. This is not unexpected, however, since in Plant's formulation the coupling of the wind to waves near the spectral peak is greater than in [4], resulting in a somewhat higher estimate of $\overline{c}$.

Figure 7 shows the WAVES dissipation values normalized as in [2] by significant height, H_s, and wind input, F_w, plotted against non-dimensional depth, z/H_s. For the data under consideration, we have estimated F_w from [5] using u_{*a} computed from [6] and [7]. The data plotted in Fig. 7 span the range $4.3 < c_p/u_{*a} < 7.4$. Over most of the depths shown they are reasonably tightly clustered and do not show a systematic dependence on wave

age. A linear regression on logarithmic variables yields a slope of approximately -1.9. The residuals are independent of c_p/u_{*a}, so that, within the uncertainty of the fit, the regression may be expressed as:

$$\frac{\epsilon H_s}{u_{*w}^2 \overline{c}} = 0.3(z/H_s)^{-2}. \qquad [9]$$

Both the linear regression and [9] appear in Fig. 7 – the two are barely distinguishable.

6. The Vertical Distribution of Dissipation

The form of the dissipation rate given by [9] is valid over a range of depths determined by the two requirements that the vertically-integrated dissipation matches the wind input, and that below some depth, the dissipation rate relaxes to the conventional wall layer result, $u_{*w}^3/\kappa z$. This latter condition enforces consistency with previous observations of wall layer behavior at sufficient depth (e.g. Soloviev *et al.*, 1988).

It will be useful at this point to review briefly the assumptions underlying our approach. We have postulated that the principal source of turbulence kinetic energy is wave breaking, and that the breaking directly injects energy to a depth, z_b, which is on the order of a wave height. We further assume that the dissipation rate between the surface and z_b has a constant value, ϵ_b, which can be estimated by evaluating [9] at z_b. We note that a similar idea was proposed by Kitaigorodskii (1984) in connection with a model for gas transfer. The energy in this "breaking layer" is transported downwards and simultaneously dissipated. However, wave breaking also transfers horizontal momentum to the near-surface currents, so that viewed on a large enough scale, the flow must be vertically sheared, but the shear may be small close to the surface where turbulence levels are high due to breaking. Hence we expect that there will be a transition depth, z_t, below which local shear production dominates the infusion of kinetic energy of breaking from above, and the turbulence energetics resemble those of flows over a rigid boundary.

As discussed previously, the vertical integral of the dissipation in the water must balance the wind input, $u_{*w}^2 \overline{c}$. The net dissipation consists of three terms: the integral of the wall layer dissipation, $u_{*w}^3/\kappa z$, from the bottom (in the present case at 12 m), to $-z_t$, (if a thermocline is present, the lower limit should be taken as the base of the mixed

layer); the contribution of [9] from $-z_t$ to $-z_b$; and finally, the integral of the constant dissipation, ϵ_b, from $-z_b$ to the surface. It is readily verified that the integral of the wall layer dissipation can be neglected with respect to the other two terms. It is interesting to note that because of the z^{-2} depth dependence in [9], the magnitudes of the two principal contributions are nearly the same (they are equal up to terms of order $O(z_b/z_t)$). The integral constraint leads to the following approximate expression for the "breaking depth", z_b:

$$z_b/H_s = 2 \times 0.3, \qquad [10]$$

which is consistent with our original physical assumption that a length scale related to the significant wave height is *imposed* by the mechanics of breaking.

Matching [9] to the conventional wall layer result, we obtain an expression for the transition depth, z_t:

$$z_t/H_s = 0.3\kappa\bar{c}/u_{*w} \simeq 3.6(\bar{c}/u_{*a}), \qquad [11]$$

where we have taken $\rho_w/\rho_a = 880$. Combining [10] and [11] gives:

$$\frac{z_t}{z_b} = \frac{\kappa}{2}(\frac{\bar{c}}{u_{*w}}) \simeq 6\frac{\bar{c}}{u_{*a}}. \qquad [12]$$

The values of z_b/H_s and z_t/H_s as defined in [10] and [11] are indicated in Fig. 7, with the range of z_t/H_s corresponding to that of the current data set. For the young, fetch-limited waves reported here, $\bar{c} \approx 0.5 \times c_p$, so that the right-hand-side of [12] is proportional to the inverse wave age. It is of interest to see how the thickness of the transition layer, z_t/H_s, varies over a wider range of wave development. To address this question, we have computed $\bar{c}/u_{*a}$ as a function of wave age, c_p/u_{*a}, using both the WAM database (Kahma and Calkoen, 1992) and the full set of WAVES data. The results are displayed in Fig. 8, and show that $\bar{c}/u_{*a}$ at first increases in proportion to wave age, reaches a maximum of roughly 7–8, and then decreases by a factor of two or more (relative to the maximum) as full development is approached. Combined with [11], these results imply that the depth of the crossover from a z^{-2} to z^{-1} behavior may be as large as $30H_s$ at some intermediate stage

of wave development. For the dissipation values shown in Fig. 7, $2.3 < \overline{c}/u_{*a} < 3.6$, giving a transition depth in the range $8.3 < z_t/H_s < 13$, or (from Table 1), $1.8 < z_t < 4$ meters.

The ratio of dissipation in the intermediate (z^{-2}) layer to the conventional wall layer estimates is given by

$$\frac{\epsilon \kappa z}{u_{*w}^3} = \frac{z_t}{z}. \qquad [13]$$

Thus our dissipation estimates rise from the conventional estimates at z_t (by definition) to a value z_t/z_b times the conventional estimates at the base of the layer of direct injection of wave breaking turbulence. This, from [12] and Fig. 8, may be as large as 45 times the wall layer estimate.

7. Discussion

The scaling on significant height, H_s, and wind input, F_w, introduced in [2] is motivated by a physical picture in which the energy flux from wave breaking is initially deposited into a relatively thin "breaking" layer adjacent to the surface. We have conjectured that the thickness of this layer, z_b is determined by the mechanics of the breaking process itself, and is proportional to the significant height of the actively wind-driven waves. Below this there is an intermediate region into which kinetic energy is transported from above by turbulence and in which the dissipation rate decays rapidly with depth as z^{-2}. This layer eventually merges into a classical wall layer at the transition depth, z_t, below which the dissipation rate decays as z^{-1}. A schematic illustration of this behavior appears in the inset to Fig. 7. Although we have shown in the preceding sections that the scenario described above provides a consistent description of dissipation beneath the fetch-limited, strongly-forced waves observed during WAVES, it is of interest to ask whether our principal results, embodied in [9]–[11], can be reliably extended to any degree of wave development. Although it remains for future experiments to provide a definitive answer to this question, some insight can be obtained by critically examining the premises underlying the arguments of the preceding sections.

First, we consider the magnitude of the dissipation (*i.e.* its vertically-integrated value). We have assumed from the start that the energy flux to the waves can be used as a surrogate

for the net dissipation in the water. As mentioned earlier, this requires that we can neglect both the direct viscous stresses on the surface, and the production of kinetic energy in the water by shear currents. The latter assumption has been verified *a posteriori* from the observed dissipation. The conventional estimate of the energy flux into the upper layer is based on the idea that the wind works directly on the surface current, U_d. This, of course, requires a viscous stress at the surface, τ_s. Although we have previously argued that τ_s is negligible when the airflow is aerodynamically rough, the conventional estimate of the energy flux, $\tau_s U_d$, provides a convenient gauge for our observed dissipation. Taking τ_s equal to the total wind stress $\rho_a u_{*a}^2$, and using Wu's (1975) estimate $U_d \simeq u_{*a}/2$, we obtain the conventional estimate of the energy flux as $\rho_a u_{*a}^3/2$. The energy flux to the waves normalized by the conventional estimate becomes $2\overline{c}/u_{*a}$. As shown in Fig. 8, this ratio is a function of wave development. It is proportional to wave age, c_p/u_{*a}, for immature waves, reaches a maximum of roughly 16 at $c_p/u_{*a} \approx 15$, and then decreases to around 3 near full development. Thus for wave age of about 15 (corresponding to $U_{10}/c_p \approx 2$), the energy flux from breaking exceeds the conventional estimate by a factor of roughly 16. The discrepancy is less for both younger and older waves. For a fixed friction velocity, c_p increases monotonically, while $\overline{c}$ first increases, and then decreases as the waves mature from very young to fully developed. This behavior reflects a change in the net wind forcing and arises because in very young seas ($c_p/u_{*a} \leq 15$) the peak of the spectrum is enhanced (Donelan *et al.*, 1985) and much of the energy input goes to the steep waves at the peak. As the waves become more mature, the enhancement diminishes until the largest waves are less steep than those in the equilibrium range and support less of the stress and energy flux. Thus in the early stages of development $\overline{c}$ tracks c_p, whereas in more mature waves the net energy flux decreases due to the reduction of the peak enhancement.

The distribution of the dissipation with depth is characterized by the breaking and transition depths, z_b and z_t. Since the bandwidth of the transition layer, z_t/z_b, is simply $6\overline{c}/u_{*a}$, the discussion above concerning the dependence of the normalized energy flux on wave age applies to this quantity as well. Our estimate of z_b is based on the assumption that the dissipation rate in the "breaking layer" is roughly constant. This leads to the conclusion that approximately half the total dissipation in the water occurs within z_b of

the surface, and yields the estimate $z_b = 0.6H_s$. Although this is slightly outside the depth range of our observations (see the inset in Fig. 7), a substantially larger value would be observable. Although we have assumed that the dissipation above z_b is constant, our conclusions are not significantly affected as long as z_b marks the beginning of a roll-off of the dissipation toward its surface value.

Because the development of our arguments depends on the choice of scaling variables, we must ask to what extent the set we have chosen is unique. Some insight into this question can be obtained by applying the arguments of the previous section to a different set of scaling variables. For example, suppose that depth is scaled by the wavenumber at the peak of the spectrum, k_p, instead of H_s, and the dissipation rate by $u_{*w}^3 k_p$ instead of F_w/H_s. Plotting the non-dimensionalized dissipation against $k_p H_s$ shows a similar collapse of the data. A fit yields a depth-dependence of $(k_p z)^{-2}$ with an overall coefficient of 8.9. However, repeating the arguments leading to [10]–[11] shows that now the transition depth, $k_p z_t$, is constant at 3.6, while the thickness of the breaking layer, $k_p z_b = 0.6 u_{*a}/\overline{c}$, is variable. Although this kind of behavior might be appropriate to describe the situation where wave-turbulence interaction over the wave layer (having a thickness of order k_p^{-1}) is the dominant production or transport mechanism, it is difficult to reconcile with our physical picture of a wave-stirred surface layer deepened by turbulent transport.

Osborn *et al.* (1992) report observations of enhanced dissipation taken under more fully developed wave conditions. In their Figure 9b, these authors show a dissipation profile that exceeds wall layer by nearly an order of magnitude close to the surface, and relaxes to values consistent with shear production at a depth of 8–10 m. Estimating their wave age, c_p/u_{*a}, to be approximately 30, we have from Fig. 8 that $\overline{c}/u_{*a} \approx 3$. Based on their estimated significant wave height of 1 m, we conclude $z_t \approx 10$ m. Since the ratio of breaking to wall layer dissipation is simply z_t/z, [13], we expect an enhancement of the dissipation by roughly a factor of 10 at a depth of 1 m, a result that is consistent with Osborn *et al.'s* Figure 9b.

Finally, it is of interest to ask whether our conclusions are consistent with what is known about the ability of the wave field to deliver fluxes of the required magnitude via

breaking. This issue has been addressed recently in two separate papers (Thorpe, 1992; Melville, 1992). Thorpe uses laboratory measurements of the rate of energy loss from quasi-steady breakers, together with field observations of the frequency of breaking to infer an energy flux into the upper layer of $E_w \simeq 3 \cdot 10^{-5} \rho_w U_{10}^3 (c_b/c_p)^5$, where c_b is the phase speed of the breaking waves. Equating this to the vertically integrated dissipation rate in the mixed-layer (Oakey and Elliot, 1982), he arrives at the estimate $c_b/c_p \simeq 0.25$. Melville takes a somewhat different approach in which he equates E_w (but reduced by a factor of 7 to account for the smaller energy flux lost by unsteady spilling breakers) to the net energy flux lost from the equilibrium range of the wave spectrum. The latter quantity is estimated using the idea, first proposed by Phillips (1985), of an approximate balance between wind input, nonlinear transfer, and dissipation. This results in an estimate of the energy flux into the water from wave breaking that is an order of magnitude larger than Oakey and Elliot's results, and leads to the condition $c_b/c_p \simeq 0.64$. Following a similar line of reasoning to that of Melville, we can equate Thorpe's E_w with our expression for the wind input, F_w, to obtain $c_b/c_p = 0.4(\overline{c}/u_{*a})^{0.2}$. This expression depends rather weakly on c_p/u_{*a} and produces ratios, c_b/c_p, in the range 0.4–0.64. The high end of the range is associated with younger waves, while the lower is characteristic of waves closer to full development. For wave ages, c_p/u_{*a}, less than 12 or so, Fig. 6 shows that c_b and $\overline{c}$ are in fairly close agreement, supporting the idea that for young waves the dissipation is quasi-local to the wind input. As full development is approached, then $c_b \gg \overline{c}$, indicating that while the direct wind forcing remains well localized at high wavenumbers, the waves participating in breaking extend over a much wider bandwidth, including most, if not all, of the rear face of the spectrum.

8. Conclusions

We have explored the rate of kinetic energy dissipation in a wind-driven aquatic surface layer. We find that the conventional view, that the dissipation rate corresponds more or less to the scaling appropriate to a turbulent wall layer, is inappropriate when the following conditions are met: (a) the airflow is aerodynamically rough so that the stress is communicated to waves of various lengths and not directly to the surface current; (b) there is wave breaking — always true when (a) occurs; (c) observations are made within a few

wave heights of the surface. In these conditions the dissipation rate decays more quickly with depth than wall layer theory would suggest. The total dissipation in the upper layers is then $\overline{\tau c}$, typically an order of magnitude greater than the conventional estimate, τu_{*a}.

Our results suggest that the wave-stirred near surface region is best described by a three layer structure: The top layer or breaking zone is a region of direct injection of turbulence from wave breaking. Its depth, z_b, is found to be roughly half H_s, the significant wave height of the wind waves, and roughly one half the total energy distribution occurs within the topmost layer. Below this lies a layer in which the energy dissipation rate decays rapidly with depth (z^{-2}), scales with wave and wind forcing parameters and eventually merges with a deeper layer of slower decay in which wall layer scaling may be appropriate. The depth of transition to wall layer, z_t, is found to increase with the normalized (by $\rho_a u_{*a}^3$) energy flux into the water column due to breaking, being related to z_b by the ratio $\overline{c}/u_{*a}$. For wave ages typical of this study (*i.e.* $U/c_p > 3$), this ratio is roughly half c_p/u_{*a} and approaches a constant of about 4 as full development is approached. Hence the thickness of the transition layer is dependent on both the significant wave height and the state of the development of the waves, and may be as much as $30H_s$ for waves of intermediate development.

Our observations reveal a region of the surface boundary layer in which the dissipation rate decays as z^{-2} and has a magnitude that is more than an order of magnitude greater than can be accounted for by shear production. We conjecture that the source of the enhanced turbulence is sporadic and patchy breaking at the surface. Boundary layers in which the turbulence is generated by shear at a rigid wall show a decay rate of the dissipation that is proportional to z^{-1}. When the flow is shear-free and the source of turbulence in continuous and uniform, as it is when imposed by the motion of a grid at the surface, the turbulent dissipation rate decays as z^{-4}. It would seem that the wave-stirred surface layer, having both imposed shear and a source of turbulence injected near the surface, leads to a novel vertical structure of the dissipation rate that is intermediate between wall layer and grid stirred, shear-free turbulence.

One of the important contributions of this work is a clear demonstration that the

conventional estimates of the dissipation rate of turbulent kinetic energy based on wall layer structure ($u_{*w}^3/\kappa z$) are too small by an order of magnitude in moderate and strong winds. Furthermore, our revised estimates of the energy flux from the wind, $\tau\bar{c}$, depends both on the stress and on $\bar{c}$, each of which are functions of the wave spectrum and its development. This underscores the absolute requirement for accurate measurements of wind and wave directional properties in studies of the dynamics of wave-stirred layers.

This work is, we believe, the first systematic attempt to assess the effects of wave breaking on the structure of natural boundary layers. The results demand new approaches to modelling the many processes of physical, biological and chemical interest that are linked to the intensity of mixing in the very near surface layers.

Acknowledgments

The participation of Y.A., E.T. and A.W. in the WAVES experiment was originally supported by the U.S. National Science Foundation under grant OCE-8418711. E.T. also acknowledges support from the U.S. Office of Naval Research under contract N00014-87-K-007 NR 083-004, and continuing support under National Science Foundation grant OCE-9301440. M.D., W.D. and K.K. were supported in part by the Panel for Energy Research and Development (Canada), and P.H. by Quest Integrated's internal R&D fund. E.T. thanks J. Trowbridge for helpful discussions. This is WHOI contribution 8509 and NWRI report 94-xxx.

REFERENCES

Agrawal, Y.C., and C.J.Belting, 1988: Laser velocimetry for benthic sediment transport. *Deep Sea Res.*, **35**, 1047-1067.

Agrawal, Y.C., E.A. Terray, M.A. Donelan, P.A. Hwang, A.J. Williams III, W.M. Drennan, K.K. Kahma and S.A. Kitaigorodskii, 1992: Enhanced dissipation of kinetic energy beneath surface waves. *Nature* **359**, 219-220.

Anis, A. and J.N. Moum, 1992: The superadiabatic surface layer of the ocean during

convection. *J. Phys. Oceanogr.*, **22**, 1221-1227.

Arsenyev S.A., S.V.Dobroklonsky, R.M.Mamedov and N.K.Shelkovnikov, 1975: Direct measurements of some characteristics of fine-scale turbulence from a stationary platform in the open sea. *Izv., Atmos. Ocean. Phys.*, **11**, 530-533.

Banner, M.L., 1990: Equilibrium spectra of wind waves. *J. Phys. Oceanogr.*, **20**, 966-984.

Birch, K.G. and J.A. Ewing, 1986: Observations of wind waves on a reservoir. Report no. 234, Institute of Oceanographic Sciences, Wormley, Surrey, England, 34 pp.

Csanady, G.T., 1984: The free surface turbulent shear layer. *J. Phys. Oceanogr.*, **14**, 402-411.

Dillon, T.M., J.G.Richman, C.G.Hansen and M.D.Pearson, 1981: Near-surface turbulence measurements in a lake. *Nature*, **290**, 390-392.

Donelan, M.A., 1978: On the fraction of wind momentum retained by waves. *Marine Forecasting: Prediction, Modeling and Ocean Hydrodynamics.* J.C. Nihoul (*ed.*), Elsiever Publishing, 141-159.

Donelan, M.A., 1990: Air-Sea Interaction. *The Sea: Ocean Engineering Science*, **9**. John Wiley and Sons, Inc., New York, 239-292.

Donelan, M.A. and J.Motycka, 1978: Miniature drag sphere velocity probe. *Rev. Sci. Instrum.*, **49**, 298-304.

Donelan, M.A. and W.J. Pierson, 1987: Radar scattering and equilibrium ranges in wind generated waves with applications to scatterometry. *J. Geophys. Res.*, **92**, 4971-5029.

Donelan, M.A., J.Hamilton and W.H.Hui, 1985: Directional spectra of wind-generated waves. *Phil. Trans. Roy. Soc. London, Ser. A*, **315**, 509-562.

Drennan, W.M., K.K.Kahma and M.A.Donelan, 1992a: The velocity field beneath wind-waves –observations and inferences. *Coastal Engineering*, **18**, 111-136.

Drennan, W.M., K.K. Kahma, E.A. Terray, M.A. Donelan and S.A. Kitaigorodskii, 1992b: Observations of the enhancement of kinetic energy dissipation beneath breaking wind waves. *Breaking waves*, M.L.Banner and R.H.Grimshaw, Eds., Springer-Verlag, 95-101.

Gargett, A.E., 1989: Ocean turbulence. *Ann. Rev. of Fluid Mech.*, **21**, 419-451.

Grant, H.L., R.W.Stewart and A.Molliet, 1962: Turbulent spectra from a tidal channel. *J. Fluid Mech.*, **12**, 241-268.

Gregg, M.C., 1987: Structures and fluxes in a deep convecting mixed layer. *Dynamics of the Ocean Mixed Layer*, Müller, P. and D. Henderson, Eds., Hawaiian Institute of Geophysics, 1-23.

Hasselmann, K., 1974: On the spectral dissipation of ocean waves due to whitecapping, *Bound. Layer Meteor.*, **6**, 107-127.

Hasselmann, K., T.P.Barnett, E.Bouws, H.Carlson, D.E.Cartwright, K.Enke, J.A.Ewing, H.Gienapp, D.E.Hasselmann, P.Kruseman, A.Meerburg, P.Müller, D.J.Olbers, K.Richter, W.Sell and H.Walden, 1973: Measurements of wind-wave growth and swell decay during the Joint North Sea Wave Project (JONSWAP) . *Dt.Hydrogr.Z., A8 (Suppl.)*, **12**, 95 pp.

Jeffreys, H., 1924: On the formation of waves by wind. *Proc. Royal Soc. London*,**A107**, 189-206.

Jeffreys, H., 1925: On the formation of waves by wind. II. *Proc. Royal Soc. London*,**A110**, 341-347.

Jones, I.S.F., 1985: Turbulence below wind waves. *The Ocean Surface - Wave Breaking, Turbulent Mixing and Radio Probing*, Y.Toba and H.Mitsuyasu, Eds., Reidel, Dordrecht, 437-442.

Jones, I.S.F. and B.C. Kenney, 1977: The scaling of velocity fluctuations in the surface mixed layer. *J. Geophys. Res.*, **82**, 1392-1396.

Kahma, K.K, 1981: A study of the growth of the wave spectrum with fetch. *J. Phys. Oceanogr.*, **11**, 1503-1515.

Kahma, K.K and C.J. Calkoen, 1992: Reconciling discrepancies in the observed growth of wind-generated waves. *J. Phys. Oceanogr.*, **22**, 1389-1405.

Kitaigorodskii, S.A., 1984: On the fluid dynamical theory of turbulent gas transfer across an air-sea interface in the presence of breaking wind waves. *J. Phys. Oceanogr.*, **14**, 960-972.

Kitaigorodskii, S.A., M.A.Donelan, J.L.Lumley and E.A.Terray, 1983: Wave-turbulence interactions in the upper ocean. Part II. *J. Phys. Oceanogr.*, **13**, 1988-1999.

Lumley, J.L. and E.A. Terray, 1983: Kinematics of turbulence convected by a random wave field. *J. Phys. Oceanogr.*, **13**, 2000-2007.

Melville, W.K., 1994: Energy dissipation by breaking waves. *J. Phys. Oceanogr., (in press).*

Miles, J.W., 1957: On the generation of surface waves by shear flows. *J. Fluid Mech.*, **3**, 185-204.

Mitsuyasu, H., 1985: A note on the momentum transfer from wind to waves. *J. Geophys. Res.*, **90**, 3343-3345.

Oakey, N.S. and J.A. Elliott, 1982: Dissipation within surface mixed layer. *J. Phys. Oceanogr.*, **12**, 171-185.

Osborn, T., D.M. Farmer, S. Vagle, S. Thorpe and M. Cure, 1992: Measurements of bubble plumes and turbulence from a submarine. *Atmosphere-Ocean*, **30**, 419-440.

Phillips, O.M., 1985: Spectral and statistical properties of the equilibrium range in wind-generated gravity waves. *J. Fluid Mech.*, **156**, 505-531.

Plant, W.J., 1982: A relationship between wind stress and wave slope. *J. Geophys. Res.*, **87**, 1961-1967.

Rapp, R.J. and W.K. Melville, 1990: Laboratory measurements of deep-water breaking waves. *Phil. trans. R. Soc. Lond.*, **A331**, 735-800.

Soloviev, A.V., N.V.Vershinsky and V.A.Bezverchnii, 1988: Small-scale turbulence measurements in the thin surface layer of the ocean. *Deep Sea Res.*, **35**, 1859-1874.

Stewart, R.W. and H.L.Grant, 1962: Determination of the rate of dissipation of turbulent energy near the sea surface in the presence of waves. *J. Geophys. Res.*, **67**, 3177-3180.

Thorpe, S.A., 1993: Energy loss by breaking waves. *J. Phys. Oceanogr.*, **23**, 2498-2502.

Tsanis, I.K. and M.A.Donelan, 1989: Wave directional spectra in mixed seas. *Proc. 2nd International Workshop on Wave Hindcasting and Forecasting*, Vancouver, Environment Canada, AES-Downsview, 387-396.

Williams III, A.J., 1985: BASS, an acoustic current meter for benthic flow-field measurements. *Marine Geology*, **66**, 345-355.

Wu, J., 1975: Wind-induced drift currents. *J. Fluid Mech.*, **68**, 49-70.

Table 1 : WAVES mean run parameters.

Run	U_{12}		H_s	T_a	T_w	f_p	$\overline{c}$	u_{*w}	u_{*a}/c_p	U/c_p
nr.	m s^{-1}	degrees	cm	$°C$	$°C$	Hz	m s^{-1}	cm s^{-1}		
85117	10.43	242.2	26.3	6.81	8.99	0.53	1.45	1.65	0.166	3.54
85159	16.00	235.0	49.0	2.47	6.73	0.41	2.06	2.97	0.231	4.19
85160	12.74	230.1	32.2	-2.86	6.55	0.48	1.71	2.09	0.191	3.92
87025	8.00	243.1	18.4	3.06	7.23	0.64	1.19	1.15	0.139	3.27
87079	7.01	231.7	16.4	14.77	7.06	0.70	0.94	1.01	0.135	3.16
87080	7.71	228.6	17.2	12.76	7.02	0.65	1.07	1.11	0.137	3.21
87082	11.13	238.4	24.9	9.03	6.84	0.53	1.37	1.75	0.177	3.79
87086	12.05	238.7	28.6	7.81	6.76	0.52	1.41	1.96	0.194	4.02
87087	11.41	246.2	28.3	7.89	6.73	0.54	1.48	1.85	0.190	3.95
87088	9.21	266.5	22.7	6.42	6.74	0.56	1.43	1.35	0.144	3.31
87091	11.54	222.0	28.2	7.62	6.58	0.52	1.50	1.85	0.184	3.86
87174	9.30	225.9	20.6	7.39	3.97	0.62	1.25	1.42	0.167	3.69
87184	9.71	245.2	21.4	2.85	4.21	0.62	1.25	1.52	0.179	3.85

Table 2: WAVES dissipation values

Run nr.	Instrument	z cm	ϵ_u cm^2 s^{-3}	ϵ_w cm^2 s^{-3}	U_d cm s^{-1}
85117	DragSph	140.0	0.21	0.36	6.08
85159	DragSph	174.0	0.90	1.27	13.78
85160	DragSph	100.0	0.59	0.64	13.56
87025	DragSph	49.6	0.92	1.06	10.51
87079	BASS	25.1	1.05	0.76	13.18
87079	BASS	65.1	0.19	0.18	6.25
87079	BASS	105.1	0.17	0.10	4.27
87079	BASS	155.1	0.09	0.08	3.51
87079	BASS	215.1	0.09	0.07	2.94
87080	BASS	65.0	0.21	0.22	7.91
87080	BASS	105.0	0.16	0.11	4.71
87080	BASS	155.0	0.11	0.08	3.37
87080	BASS	215.0	0.12	0.08	2.73
87082	BASS	60.6	0.59	0.64	12.88
87082	BASS	100.6	0.21	0.26	7.65
87082	BASS	150.6	0.11	0.13	4.40
87082	BASS	210.6	0.07	0.07	2.56
87086	BASS	15.3	46.51	14.66	35.20
87086	BASS	55.3	1.70	1.43	20.83
87086	BASS	95.3	0.81	0.98	13.48
87086	BASS	145.3	0.40	0.37	9.14
87086	BASS	205.3	0.08	0.13	5.33
87087	DragSph	51.6	0.70	0.49	18.08
87087	BASS	19.2	30.68	6.51	31.86
87087	BASS	59.2	1.26	1.11	18.38
87087	BASS	99.2	0.56	0.65	11.44
87087	BASS	149.2	0.24	0.18	7.89
87087	BASS	209.2	0.02	0.04	4.55
87088	DragSph	51.5	1.10	1.85	14.56
87088	BASS	59.1	0.45	0.48	12.98
87088	BASS	99.1	0.10	0.17	7.35
87088	BASS	149.1	0.03	0.04	4.12
87091	BASS	59.9	0.74	0.68	17.79
87091	BASS	99.9	0.35	0.41	11.44
87091	BASS	149.9	0.11	0.10	7.07
87091	BASS	209.9	0.02	0.03	4.19
87091	LDV	30.0	—	0.54	—
87091	LDV	40.0	—	0.33	19.08
87091	LDV	50.0	—	0.19	15.77
87174	DragSph	61.9	1.41	—	10.29
87184	DragSph	62.5	1.12	1.85	10.42

N.B. LDV runs 1/4 of length of BASS/DragSph runs.

FIGURES

1. Photograph of the Canada Centre for Inland Waters research tower.
2. Map of Lake Ontario showing the site of the WAVES experiment.
3. a) Spectra from BASS showing horizontal and vertical velocities with $\omega^{-5/3}$ regions. The dashed line is the vertical velocity predicted from the measured wave height using linear theory. b) Spectra of a) multiplied by $\omega^{5/3}$, showing the existence of inertial subranges.
4. Dragsphere spectra showing horizontal and vertical velocities with $\omega^{-5/3}$ regions. The dashed line is the vertical velocity predicted from the measured wave height using linear theory. b) Spectra of a) multiplied by $\omega^{5/3}$, showing the existence of inertial subranges.
5. Turbulent kinetic dissipation rate ϵ from horizontal versus ϵ from vertical velocity spectra using frequencies above the wave band (BASS).
6. The ratio $\overline{c}/c_p$ versus inverse wave age, u_{*a}/c_p, where $\rho_a u_{*a}^2 \overline{c}$ is the energy flux from the wind to the waves.
7. The normalized dissipation rate, $\epsilon H_s/u_{*w}^2 \overline{c}$ versus dimensionless depth, z/H_s. o and $\times$ represent data calculated from horizontal velocity fluctuations S_{uu}; the remaining points are via S_{ww}. z_b and z_t (on the right hand ordinate) are the length scales of the breaking zone and the transition depth to wall layer, with the range of the latter due to variations in $\overline{c}/u_*$ in the data set. The dashed line is the regression line to the data set in the range covered by the line. The solid line is equation [9]. The inset shows the data (only one set of points per instrument, all denoted with o), the wall layer scaling for the data (dashed) and the proposed vertical structure: constant dissipation down to z_b, $(z/H_s)^{-2}$ scaling to z_t with a transition to wall layer scaling at greater depths. The two (dashed) wall layer lines show the possible range for the data in these coordinates.
8. The ratio $\overline{c}/u_{*a}$ versus wave age, c_p/u_{*a}.

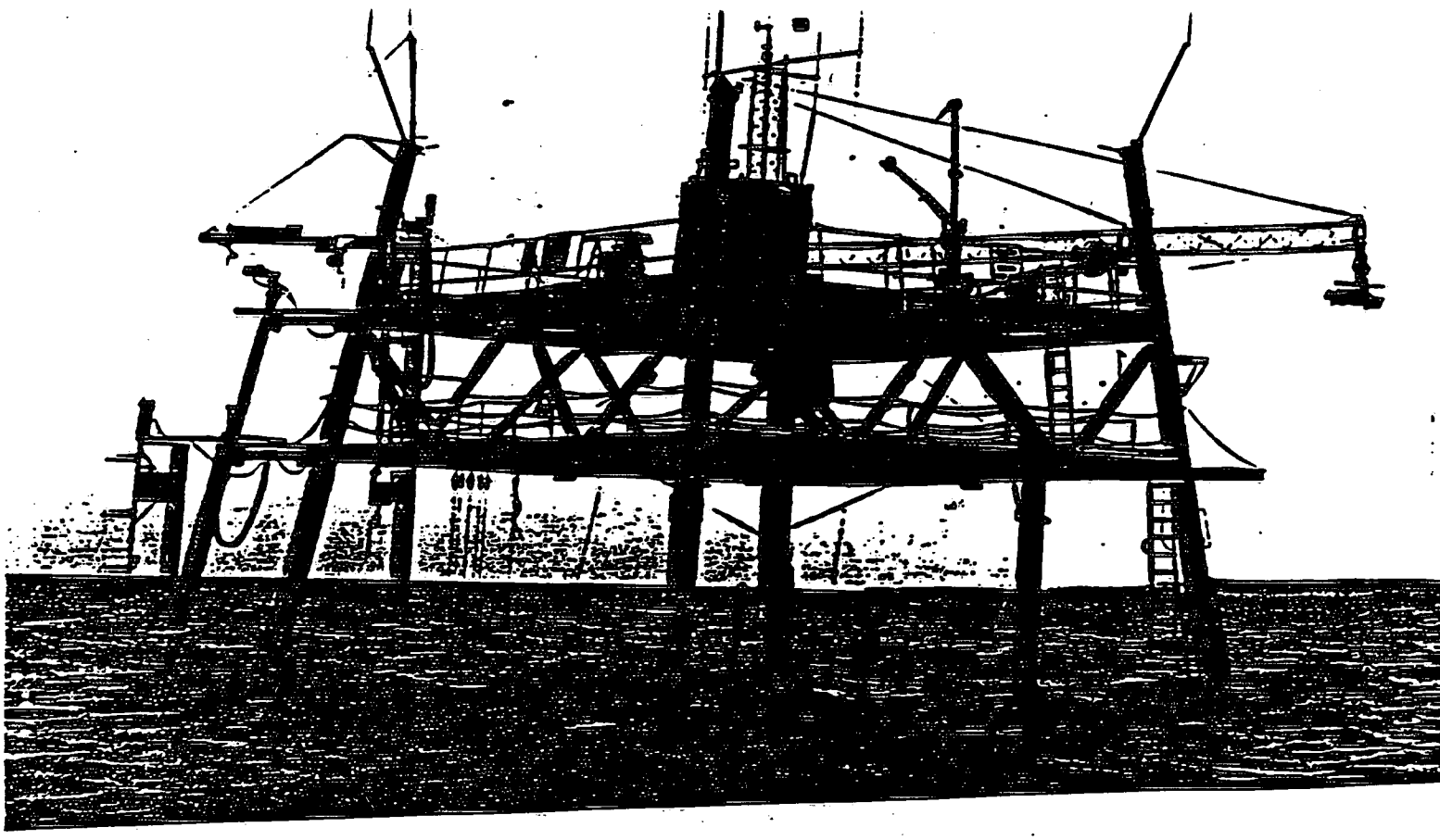

Figure 1: CCIW tower, Lake Ontario.

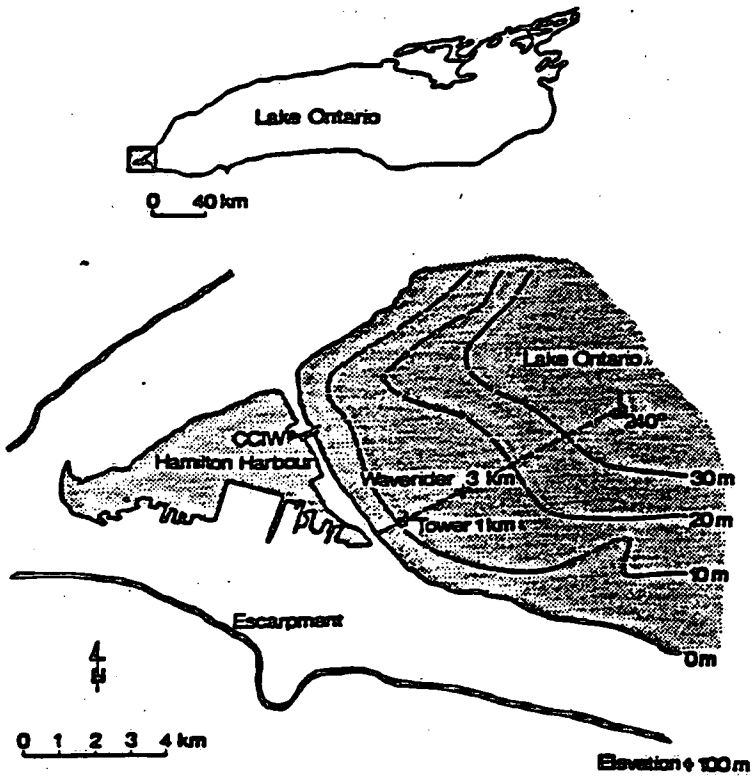

Figure 2: Map indicating tower location.

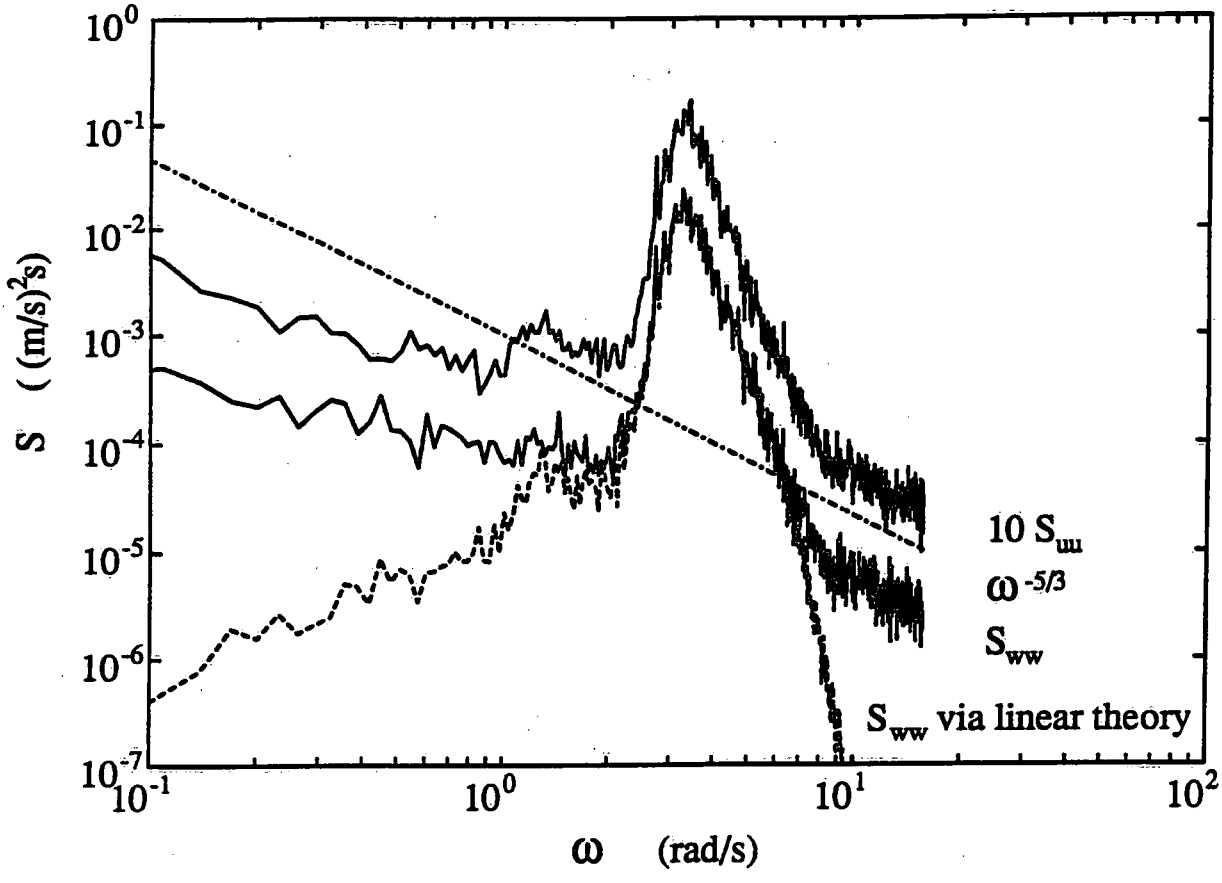

Figure 3a

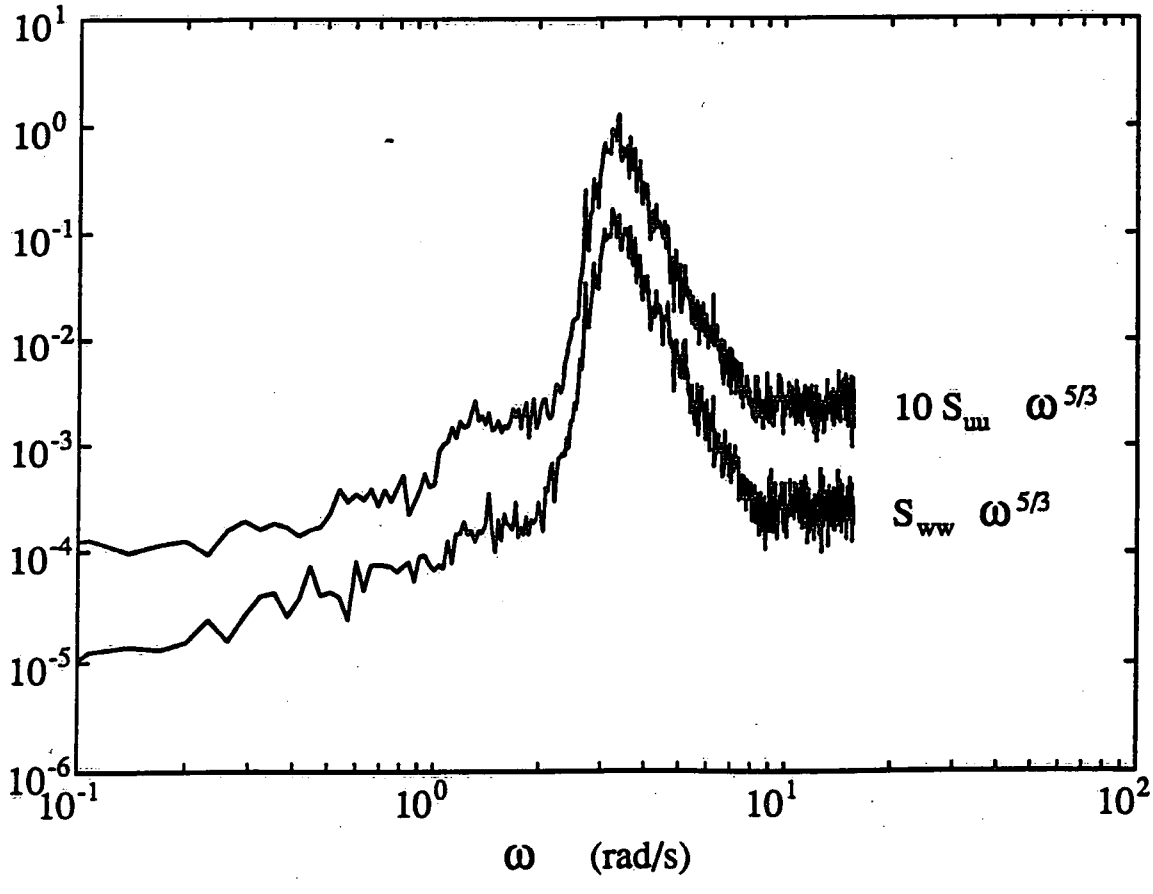

Figure 3b

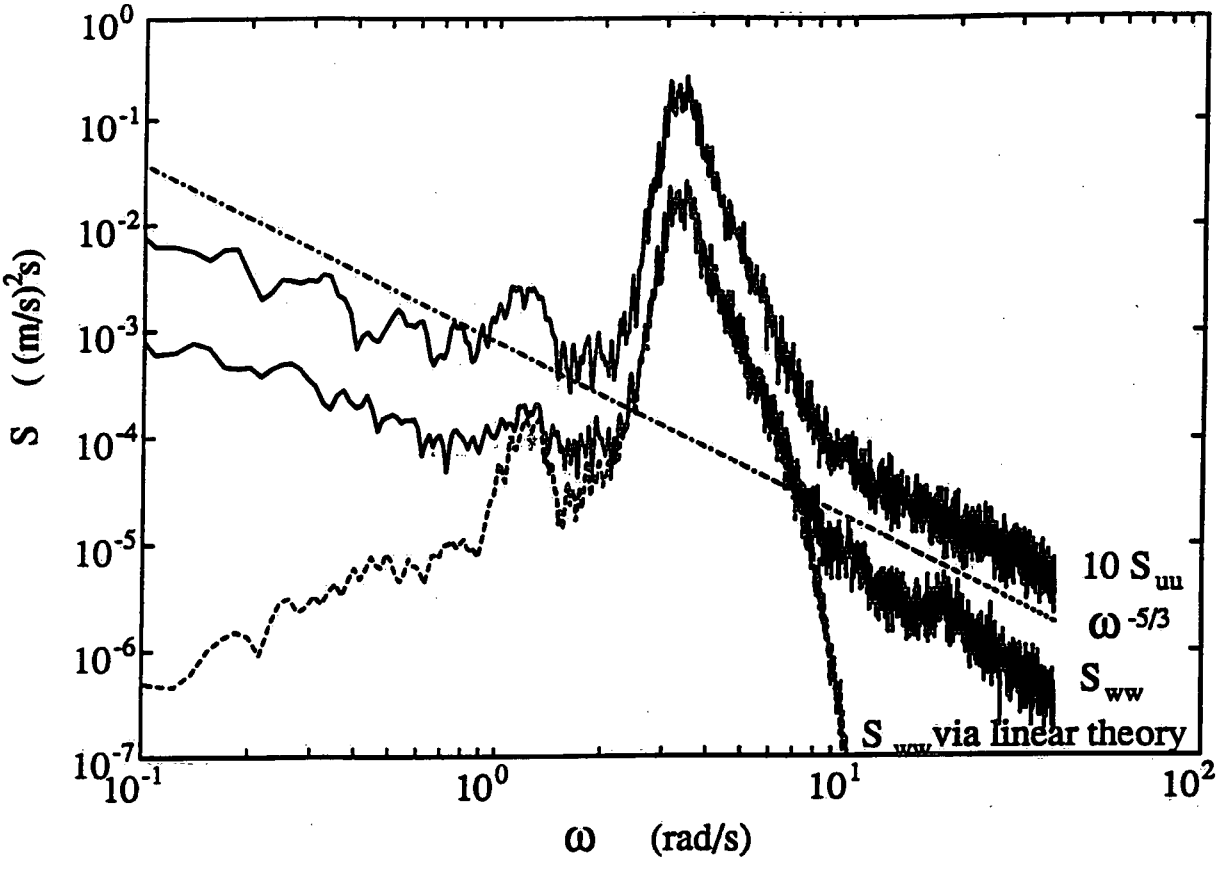

Figure 4a

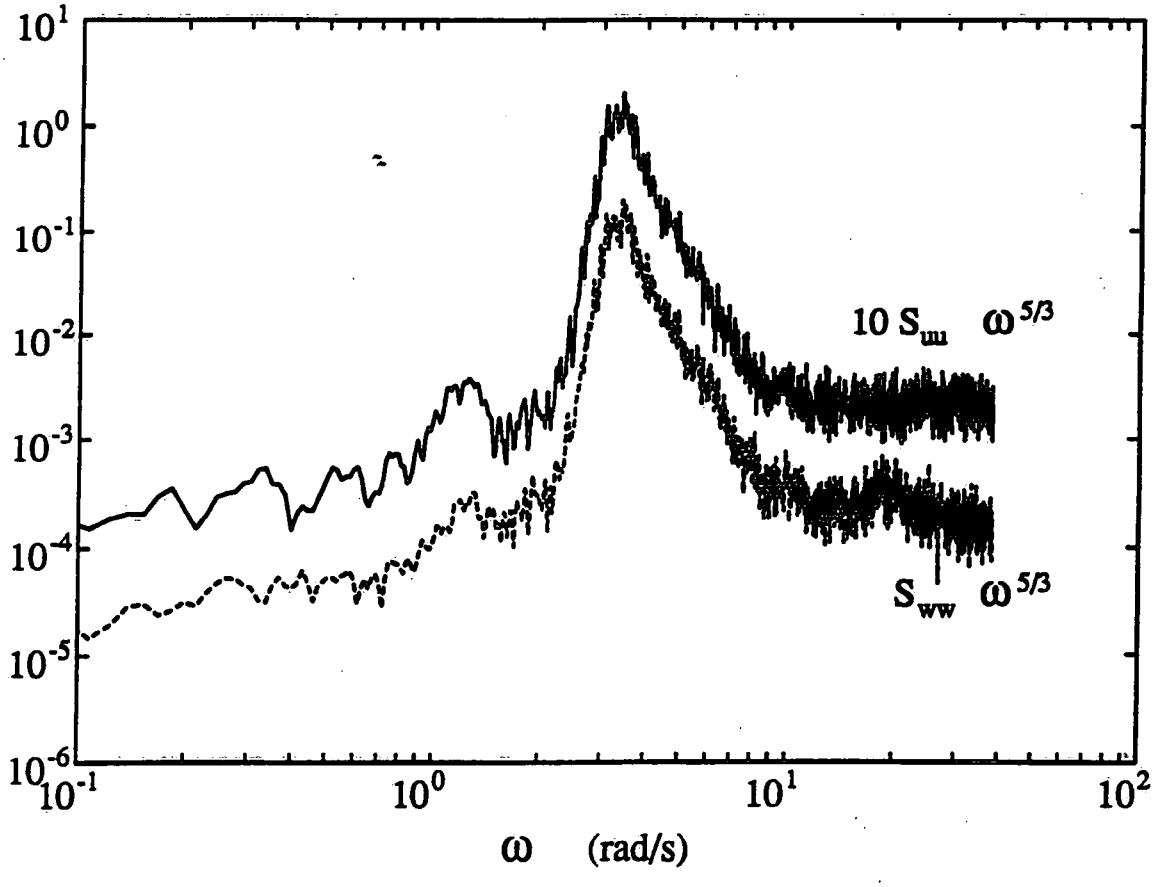

Figure 4b

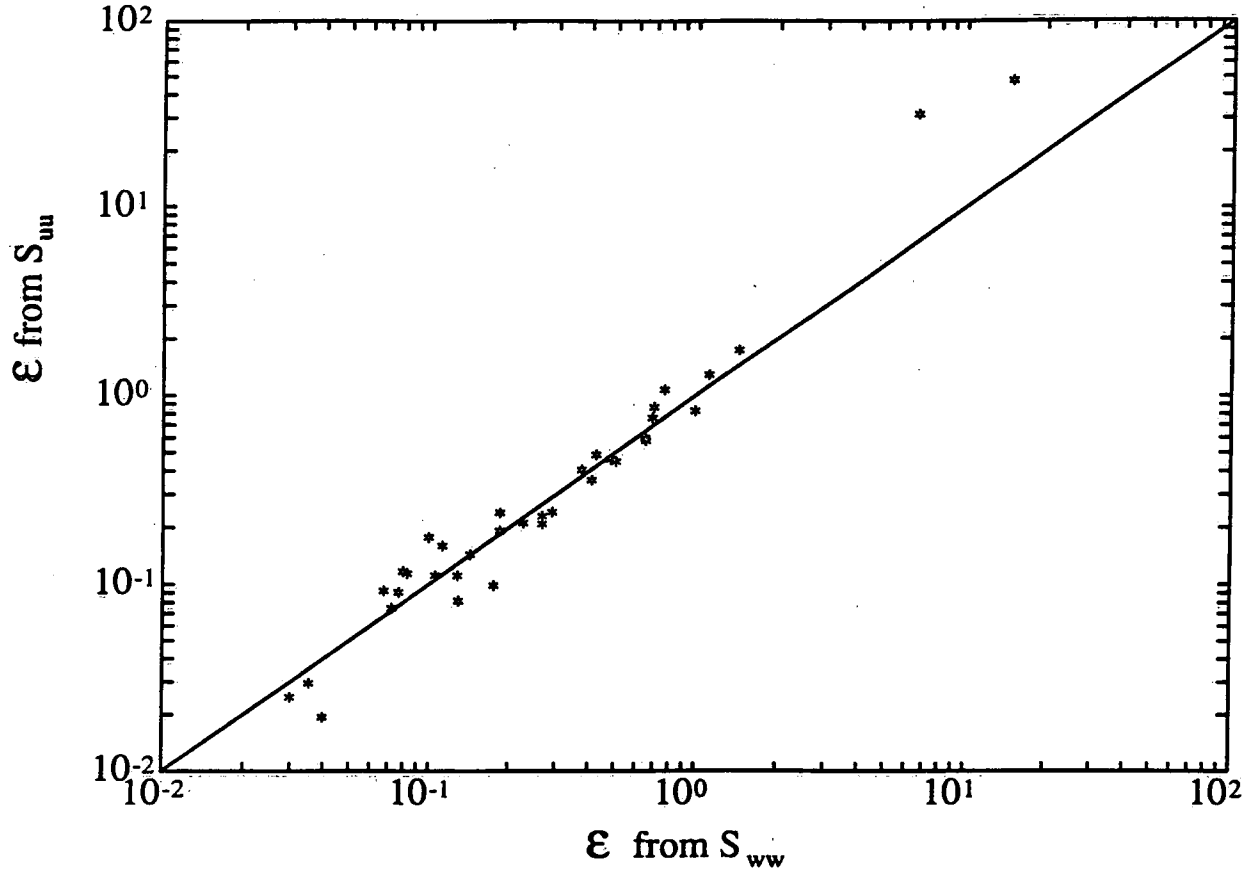

Figure 5

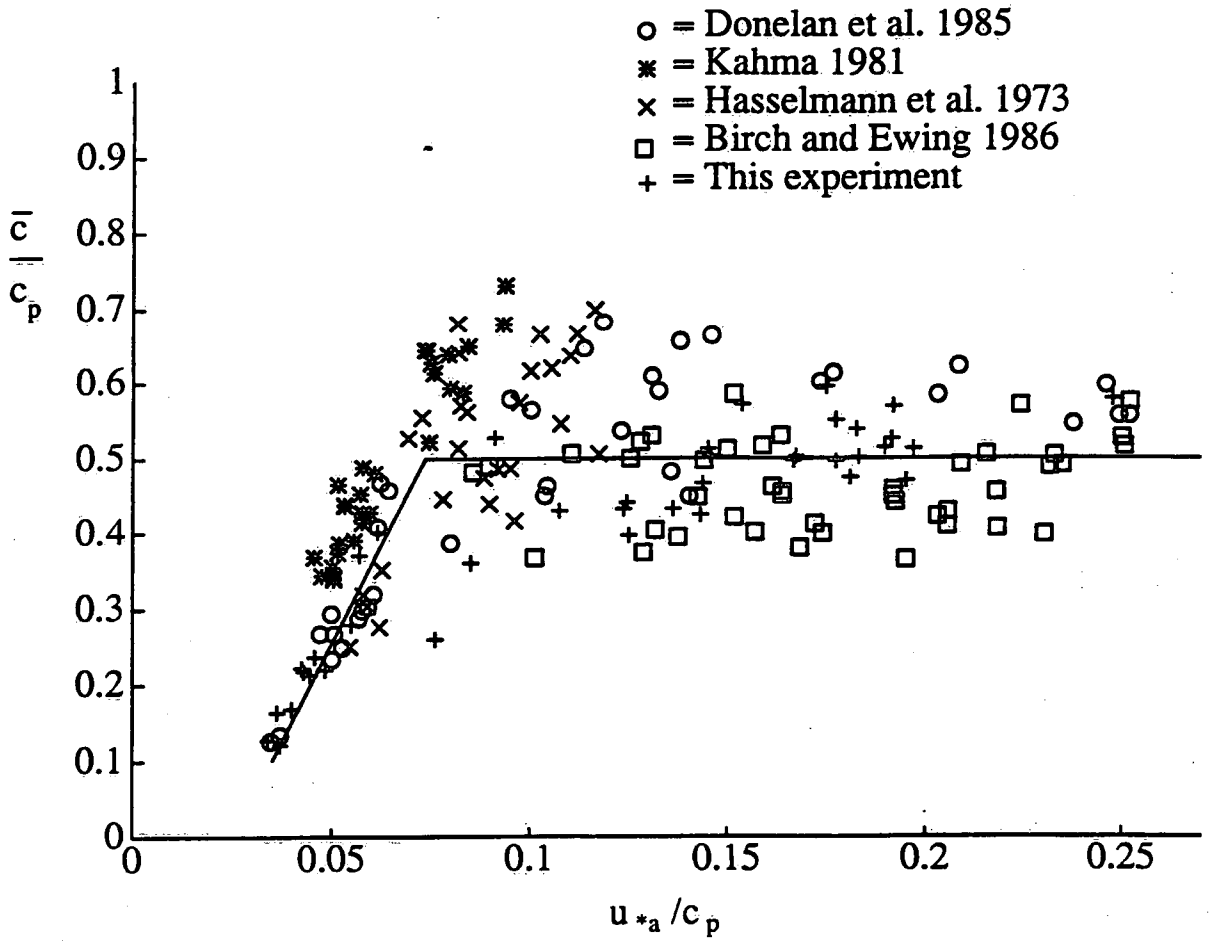

Figure 6

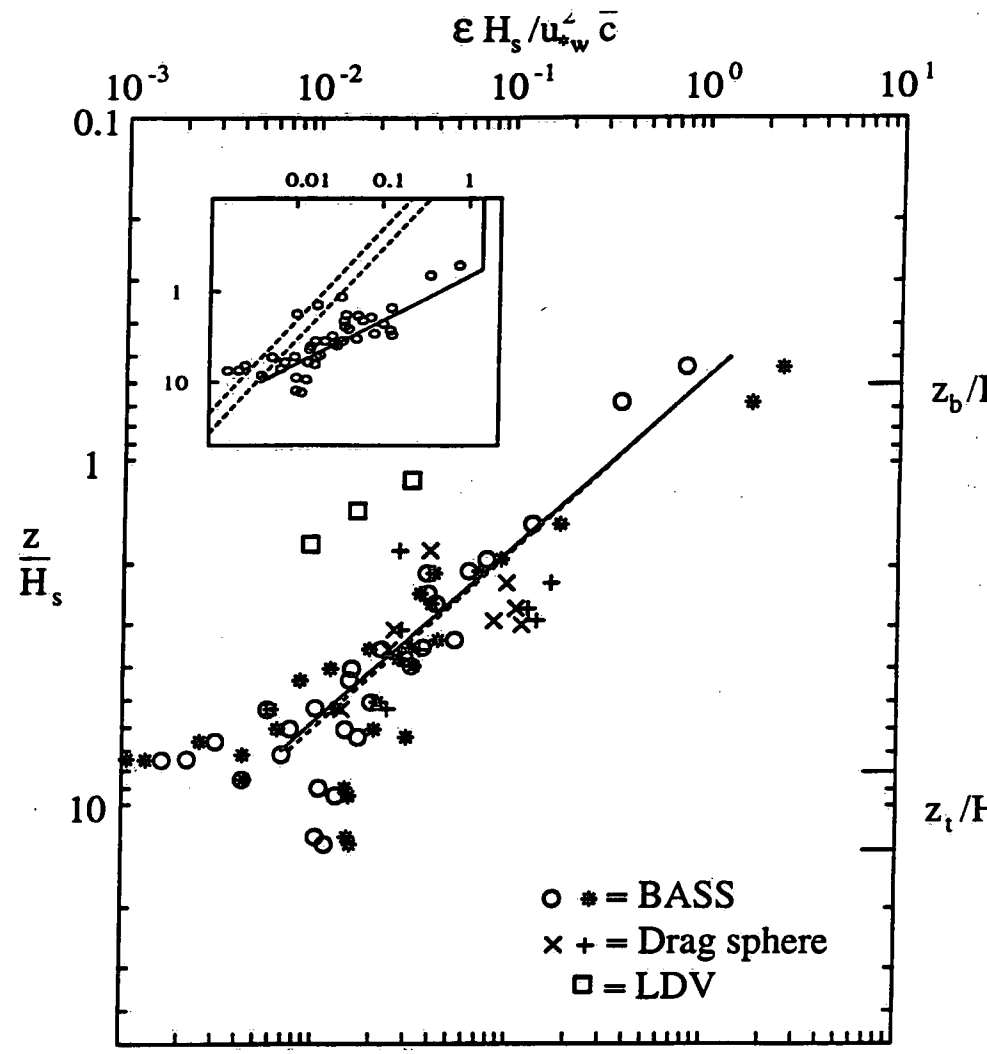

Figure 7

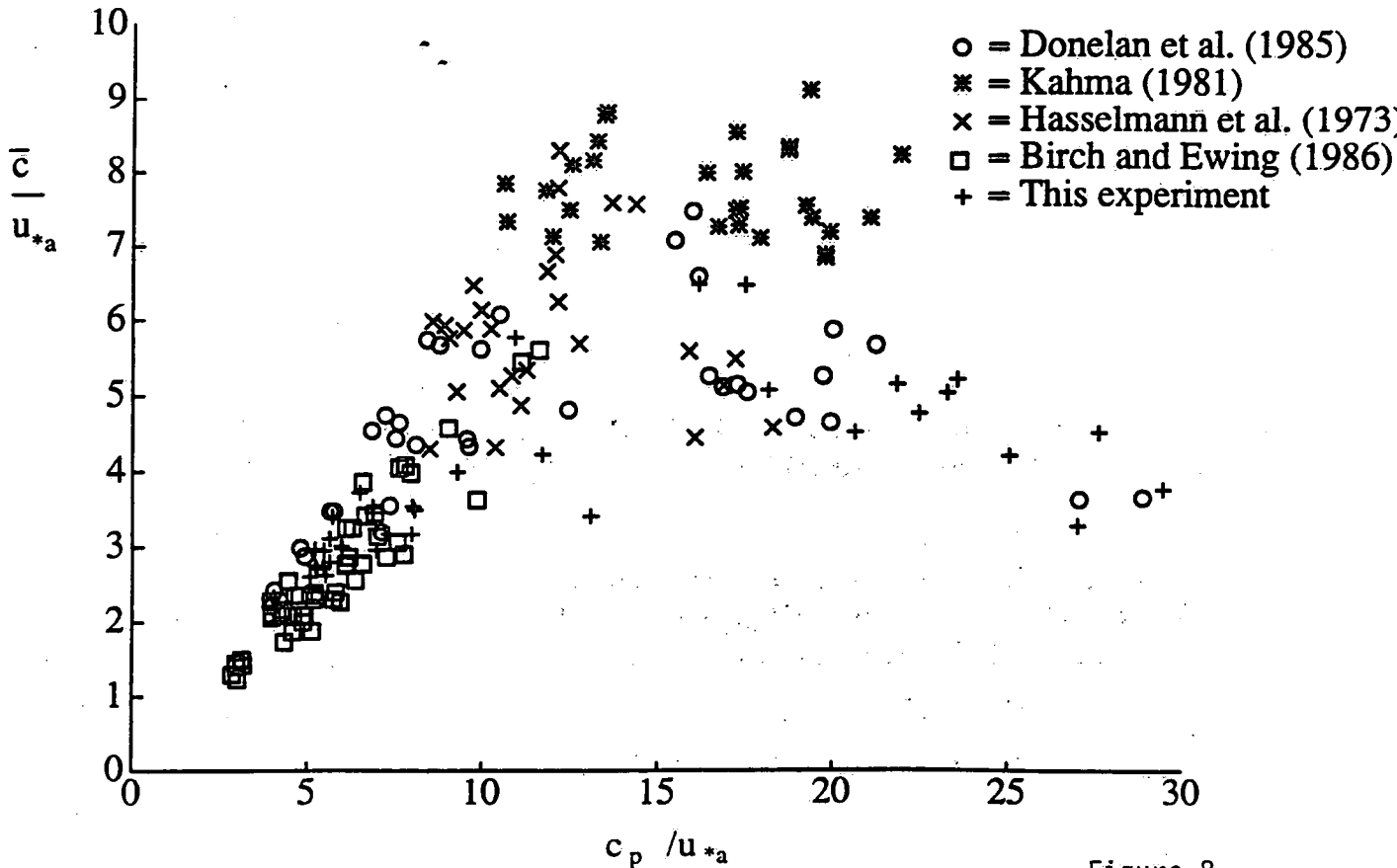

Figure 8

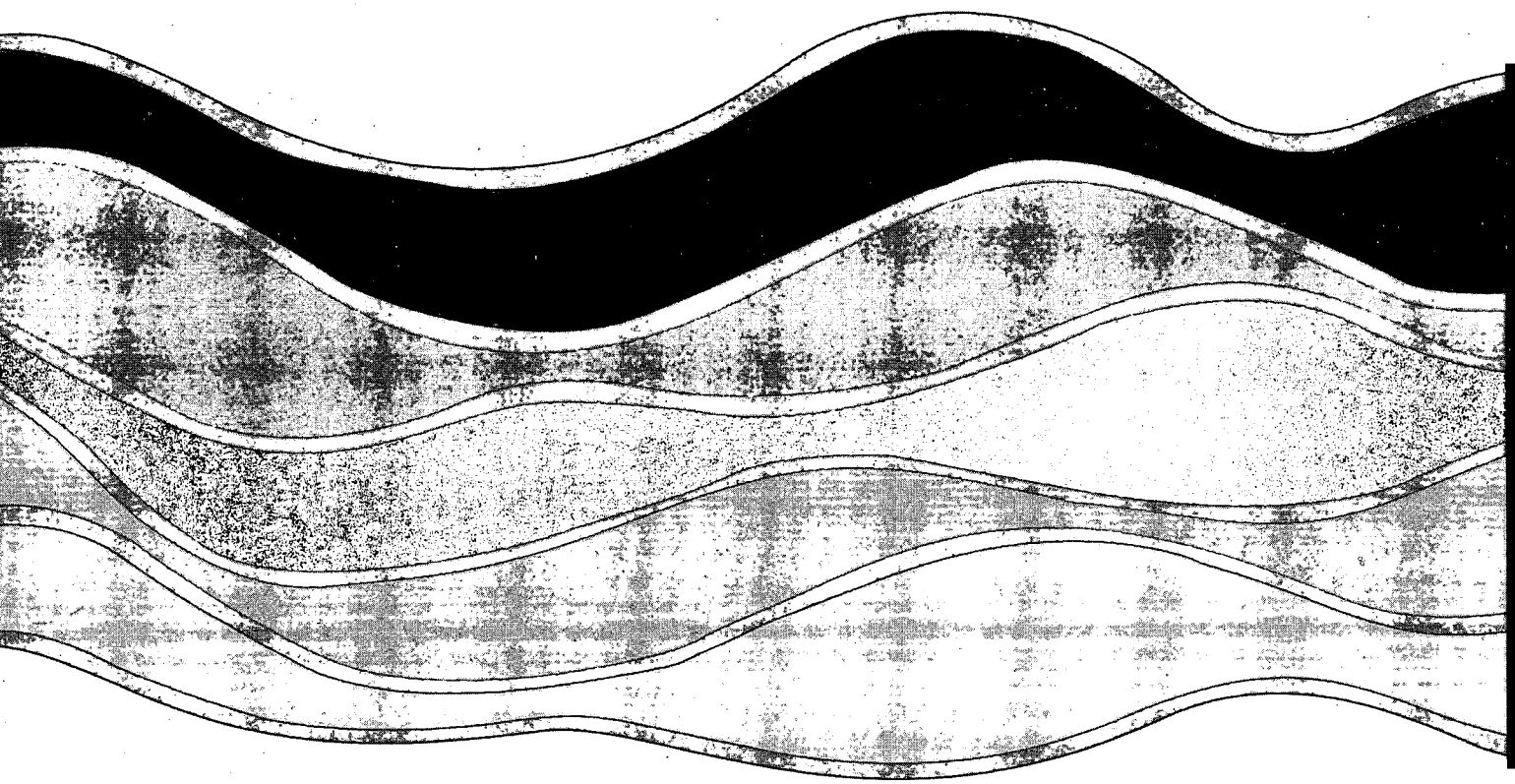

NATIONAL WATER RESEARCH INSTITUTE
P.O. BOX 5050, BURLINGTON, ONTARIO L7R 4A6

Environment Canada Environnement Canada

Canada

INSTITUT NATIONAL DE RECHERCHE SUR LES EAUX
C.P. 5050, BURLINGTON (ONTARIO) L7R 4A6